ELECTRIC AND INERTIAL FORCES IN PESTICIDE APPLICATION

Thesis for the Degree of Ph. D.

MICHIGAN STATE COLLEGE

Henry Dittimus Bowen

1953

This is to certify that the

thesis entitled

Electric and Inertial Forces

in Pesticide Application

presented by

Henry D. Bowen

has been accepted towards fulfillment
of the requirements for

Ph. D. degree in Agricultural Engineering

Walter M. Carleton
Major professor

Date Nov. 21 1953

ELECTRIC AND INERTIAL FORCES IN PESTICIDE APPLICATION

By

Henry Dittimus Bowen

A THESIS

Submitted to the School of Graduate Studies of Michigan State College of Agriculture and Applied Science in partial fulfillment of the requirements for the degree of

DOCTOR OF PHILOSOPHY

Department of Agricultural Engineering

Year 1953

HENRY DITTIMUS BOWEN AN ABSTRACT

The author presents the problems involved in work dealing with the deposition of small particles on plant surfaces. It is stated that the low recovery efficiency resulting from the use of current dusting and spraying machinery cannot be improved substantially without further information regarding the nature of the forces active in particle deposition. A theoretical approach is considered to be desirable because present evaluation techniques are considered inadequate to provide meaningful data in the light of the many physical phenomena that may effect both deposition and sticking after the particle strikes the surface.

The author proposes to obtain the order of magnitude of forces active in particle deposition and specifically the relation between electric and inertial forces that may be active within the plant regions. It is believed that this quantifying of the magnitudes of the forces will then allow the development of a greater understanding of the deposition and adherence problems. Also the theoretical results will allow more pointed investigations to be set up for the testing of ideas relative to improving machinery and techniques for particle deposition.

Instruments now available for measuring electric fields or potentials have relatively large capacitances and inertias associated with them. The volume distributions of charge that results when charged dust is blown into the inner regions of

a plant contains such a small amount of charge and the distributions change so rapidly that present day instruments disturb the fields being measured greatly, and are not able to follow the rapid changes of the field. Because of the above situation, a measureable field was calculated by two methods and also measured. The correlation being very good, it was concluded that calculation methods and assumptions used could be considered valid for calculations of those fields that could not be measured. A method of calculating the force produced on charged particles near small conducting disks at zero potential (approximating plant leaves) is given.

A study is made of the inertial forces produced and the resulting path of an uncharged particle that is described when an airstream carrying the particle is deflected by a surface.

A comparison is made between inertia, electric, and gravity forces for several electric fields. The results indicate that electric forces are generally small compared to inertia forces and are comparable in magnitude to gravity forces for uniform charge distributions. However, under actual conditions the forces may be considerably greater than calculated due to redistribution of charges in the cloud so that the charge density is no longer uniform.

The above results have shown that the electric forces developed within a plant region depend both on the charge density

and the thickness of the cloud blanket near the depositing surface. This explains partially the inability of workers to transfer laboratory work on single surfaces and spheres with thick blankets of cloud surrounding them to the field where there exists much closer spacing of deposit surfaces with resultant thinner cloud blankets and thus lower forces.

Henry Dittimus Bowen

candidate for the degree of

Doctor of Philosophy

Final examination, November 21, 1953, 9:00 A.M., Room 218, Agricultural Engineering Building

Dissertation: Electric and Inertial Forces in Pesticide Application

Outline of Studies

Major subject: Agricultural Engineering
Minor subjects: Mathematics, Physics

Biographical Items

Born, October 16, 1921, Bear Lake, Michigan

Undergraduate Studies, Michigan State College, 1946-49

Graduate Studies, Michigan State College, 1950-52

Experience: Graduate Assistant, Michigan State College, 1950-52, Assistant Professor, North Carolina State College, Agricultural Engineering Department 1953

Member of Tau Beta Pi, Phi Kappa Phi, Society of the Sigma Xi, Farmhouse Fraternity and American Society of Agricultural Engineers

TABLE OF CONTENTS

Page

LIST OF FIGURES

LIST OF TABLES

ACKNOWLEDGMENTS

The author wishes to express his sincere appreciation to Professor A. W. Farrall, head, Agricultural Engineering Department, Michigan State College, for his continued faith in the work and the provision of a research assistantship provided by the Rackham Foundation, also to the Rackham Foundation in granting the research assistantship for carrying out the work on "Electric and Inertial Forces in Pesticide Application".

Sincere thanks are extended to Professor I. O. Ebert, Electrical Engineering Department, Michigan State College, for his early interest in the project and help with equipment, to Professor Henry Parkus, Mathematical Department, Michigan State College, for his help in understanding the electric fields, to Dr. R. C. Bullock, Mathematical Department, North Carolina State College, for his help in setting up the equation of motion for the inertia force analysis, to Professor A. E. Mitchell, Horticulture Department, Michigan State College, for his interest, and to all other instructors of math and physics that have contributed to the background in making this study possible.

The author wants to express his thanks to all of the men in the Research Department at Michigan State College, especially

Mr. James Cawood, for continued help in construction of equipment.

The author is especially grateful to his major professor, Dr. W. M. Carleton, for his guidance and continued encouragement throughout the period in which this study was made.

Special appreciation is felt toward Mr. W. E. Splinter for his unselfish help throughout the planning and execution of all of the work in regard to the electrical field measurements.

Sincere thanks are due Professor G. W. Giles, head, Agricultural Engineering Department, North Carolina State College, for his interest in this project, and also to the other members of the Agricultural Engineering Department who helped on the drawing of pictures and assembling of this thesis.

The author wishes to express his appreciation to his wife, Mrs. Jean Bowen, for her encouragement and the typing of this thesis.

INTRODUCTION

Nature of the Study

The following work deals with the nature and magnitude of the several forces usually active to some degree in the depositing of agricultural dusts and sprays on to crop plant surfaces. The forces studied in some detail are the electric and inertial. Gravity and thermal fields are mentioned but no thorough study has been made.

Purpose of the Study

The study was undertaken to develop a greater understanding of the nature of the several forces active in the deposition of agricultural crop sprays and dusts in order that more efficient machinery and techniques for application could be developed.

Although spraying and dusting operations have been carried on for many years and the need for pest control has increased yearly, the equipment for applying pesticides is yet woefully inefficient. From work carried out by Bowen and others (4), it is believed that with present techniques and machines the dust recovery seldom exceeds 10 to 20 percent under day time

operation (windy and no dew). Dust recovery refers to the amount of dust actually deposited on the plant surfaces as compared to the amount discharged by the dusting machine.

According to Brooks (5) when dusting tomato vines with calcium arsenate by airplane, 50 to 60 percent of the dust drifts off the tract (200 ft. width) of dusting interest. This waste dust serves to contaminate pasture and forage fields on the downwind side of the tract. Only a fraction of the dust that remains on the tract is actually deposited on the plant, and often that is not uniformly spread over the plant surfaces.

History of the Study

The agricultural engineer has been greatly hampered in the past in working with dust and spray machinery because of two major obstacles. The first is inadequate evaluation techniques. The few evaluation techniques now available to him have either been unreliable or very expensive and have always required too much time. For this reason perhaps more than any other, the profession has not made any major advances in pesticide machinery.

The second obstacle has been an almost complete lack of information as to the relative importance and nature of the forces that act to deposit dust or spray particles on to plant

or other surfaces.

The first problem is being studied by workers in several public experimental agencies, but to the author's knowledge no one in the profession is working to increase the information regarding the forces acting to deposit particles onto plant surfaces. It is inconceivable to the author that significant advances will be made without more information about the forces acting.

The author and co-workers spent some three years of continuous effort directed toward improving dust recovery by utilizing the electrostatic forces produced when charged dust is blown into the plants. An increase in dust recovery of some 100 percent was encountered, but biological results have not shown a corresponding improvement in plant protection. It has not been determined why this is the case since evaluation techniques available have not indicated the relative amounts of all the various chemical constituents that are deposited on the plants. The same problem of evaluation has plagued the entomologist and plant pathologist, and as a result often all that is known about a pesticide is that if a certain quantity is mixed with a carrier and then blown or sprayed onto the plants at a certain rate, the pests will sometimes be eliminated. Ultimately, however, an improved recovery efficiency will result in improved pest control or increased economy. To this end it is desirable to increase recovery.

The workers in electrostatic dusting soon realized that elementary physics explanation of induced charges on the plants attracting the charged dust cloud gave no indication whatever of the magnitudes and directions of the forces in a charged dust cloud. It was impossible to develop a clear concept of the physical processes being carried out because of the complete lack of information as to the magnitudes of the inertial and electric forces occurring.

Definition of the Problem

The problem is to determine the magnitude and directions of the forces active in dust clouds.

Limiting the Problem

The problem is of considerable complexity and each of the two more important forces merit an individual treatment beyond what was possible by considering the two. However, since there was such a lack of information of the forces of either phase it was believed desirable to devote a portion of the time to each force in order to determine its relative importance. It is hoped that the material presented will stimulate other workers in the field to take up those portions that need further clarification and that in time the force systems will be fully

understood by all workers in the field. For the reasons stated above, it has been considered proper to determine the order of magnitudes of the forces and not try to determine the exact forces of a given system.

ELECTRIC FIELDS IN CHARGED DUST CLOUDS

Discussion of Electric Fields in General

Electric fields refer to those regions of space in which an electric charge placed therein would have a force exerted upon it. An electric field may be present in a region even though actual charges are not present. An electric field in the macroscopic sense need not be present in a region where charges of both signs are present in equal numbers and uniformly dispersed throughout the region. Local fields will be present in this case, however. In the case where there are charges of one sign only dispersed throughout a region there will always be an electric field within the region. The magnitude of the field will depend upon the distribution of the charges and the proximity and magnitude of charges on the neighboring boundaries of the system. The field intensity is the negative gradient of the potential and, therefore, may be determined if the potential distribution can be found.

The field intensity is the force that would be exerted upon a unit positive charged particle, if that particle were placed in the field. Thus the force experienced by any charged particle due to the electric field can be calculated by knowing the magnitude and sign of the charge and the field intensity.

Calculated Distributions of a Spherical Cloud of Charged Dust

Direct measurement of the electric fields occurring in regions surrounding plants in the field when a charged dust cloud is blown into the region is of great difficulty. The difficulty comes as the result of two conditions that are more or less incompatible. Available instruments have relatively large electrical capacities and inertias, and the electrical quantities being measured are generally very small and dissipate very quickly. In most cases the capacity of the instrument and its necessary leads is as large or is larger than the capacity of the system being measured. This, of course, violates the rule that a measuring system should not unduly disturb the values of the quantity being measured. Secondly, the electric fields formed by a dust cloud and any conducting boundaries are quickly dissipated both by the electric forces set up and by diffusion processes. The relatively large inertia of the instrument movement does not allow the needle to follow the fast changing fields.

In attempts at direct measurement of charged smoke in a pyrex boiling flask, the potential distribution proved to be essentially constant all over the volume of the flask within the time (about one minute) required to measure the potential at two different positions.

In order to be confident of the calculations for fields that are impossible to measure with today's equipment, it is

required that a measureable field be both calculated and measured. The measured field should show a reasonable correspondence to the calculated field for the same boundary conditions and charge distribution. The field selected for this purpose was that of a spherical cloud. The calculations for a uniform charge density are worked out in Appendices I and II. The calculations in Appendices I and II are for a spherical cloud surrounding a metal sphere at ground or zero potential with a zero boundary at infinity. Other cases using several values for the potential on the sphere and a zero potential at the outer boundary of the cloud have been worked out in the text.

The ultimate goal is to determine the electric field forces acting on charged dust particles. These forces may be obtained from the product of the electric field intensity and the particle charge. Either the electric field intensity or the electric potential may be calculated using superposition methods. However, it was somewhat easier to measure the potential distribution (from which field intensity could be deduced) than to measure the field intensity directly. It is also believed that the potential distribution concept of electrostatic deposition is a valuable contribution to the understanding of the phenomena. For the above reasons the calculations of the potential distributions of the several cases will be compared with the measured potential distributions. If these prove to be substantially in agreement, then the field intensity (negative of first derivative of potential)

will be derived from the calculated equations of potential distribution.

The initial calculations of a homogeneous cloud enclosing a grounded sphere were made using a Kelvin transformation or inversion within a sphere. Because it was not certain at all in the investigator's mind that the field could be satisfactorily measured, a second calculation of the same problem using superposition methods was made. Exactly the same equations resulted from both methods and since the superposition method was considerably less complex and would be more easily understood by other workers in the profession, the superposition method is the only one presented in the text. For the special case of a uniform cloud surrounding a grounded conducting sphere and a zero boundary at infinity both the superposition and Kelvin transformation methods are given in Appendices II and III. Graphical additions of several fields are presented in the body and actual calculations are presented in Appendix I.

The method of superposition has the advantage that it may be used for synthesis of any complex field when all of the simple components of the field can be calculated or measured. In fact, by knowing the boundary conditions, certain of the fields may be found quickly by a trial solution without resorting to the simultaneous solutions of several equations. It is hoped that the superposition approach will lead other workers to a better appreciation of the actual nature of the

electric fields and will demonstrate the method in which geometric arrangement of boundaries may be applied to produce the desired fields with a dusting machine for field use.

A graphical solution for the case of a cloud with a grounded sphere within it will be made. The first calculation is for a cloud with a zero potential at infinity of the type calculated in Appendices I and II.

From Appendix I the potential of a charged spherical cloud with a uniform charge density ρ and a radius b is equal to

$$U_\rho = -2\pi\rho\rho^2/3 + 2\pi\rho b^2 \ldots\ldots\ldots \rho \leq b \qquad (1)$$

where ρ is the distance from the center of the cloud.

$$U_\rho = 4\pi\rho b^3/3\rho \ldots\ldots\ldots\ldots\ldots\ldots \rho \geq b \qquad (2)$$

The following table gives the value of $U_\rho/\pi\rho$ from $0 \leq \rho \leq 5$, where b = 3

TABLE I

POTENTIAL OF A UNIFORMLY CHARGED CLOUD VS DISTANCE FROM CENTER

ρ In Units	$U_\rho/\pi\rho$ In Units
0	18.00
1	17.33
2	15.33
3	12.00
4	9.00
5	7.20

Figure (1a), page 19, shows the cross-section of the uniform cloud of charge density $+\rho$. Figure (1b), page 19, shows the potential distribution along an extended horizontal diameter of the cloud.

If a metal sphere of radius a is to be placed in the center of the cloud, the metal sphere will displace some of the cloud, thus leaving a hole in the cloud. This will change the potential by a definite amount due to the absence of the charge originally in the space occupied now by the metal sphere. We must then fashion a cloud with a hole within it of a size that the metal sphere will just fit into. This is most easily done by adding a small cloud of $-\rho$ charge density (having a volume equal to the metal sphere) to the large cloud. The small negative cloud superposed at the center of the positive cloud leaves a net charge of zero and thus makes a hole in the large cloud from the charge distribution standpoint. This negative cloud also subtracts from the potential throughout the exterior of the cloud. The potential of the small negative cloud is given by

$$U_e = 2\pi\rho\rho^2/3 - 2\pi\rho a^2 \ldots\ldots\ldots \rho \leq a \qquad (3)$$

$$U_a = -4\pi\rho a^3/3\rho \ldots\ldots\ldots\ldots \rho \geq a \qquad (4)$$

Figure (2a) and Figure (2b), page 19, give the cross-section of a small negative cloud and the potential distribution along a horizontal diameter of the small negative cloud respectively.

The sum of the large positive cloud and the small negative cloud is as follows

$$U_{a+b} = 2\pi\rho(b^2 - a^2) \quad \rho \leq a \qquad (5)$$

$$U_{a+b} = -2\pi\rho\rho^2/3 + 2\pi\rho b^2 - 4\pi\rho a^3/3\rho \quad a \leq \rho \leq b \qquad (6)$$

$$U_{a+b} = 4\pi\rho(b^3 - a^3)/3\rho \quad \rho \geq b \qquad (7)$$

The following table gives values of $U/\pi\rho$ for the hollow cloud. Figure (3a), page 19, shows the cross-section of charge density of a hollow cloud. Figure (3b), page 19, shows the potential distribution along an extended horizontal diameter of a hollow cloud.

TABLE II

POTENTIAL OF A HOLLOW CLOUD
VS THE DISTANCE FROM CENTER

ρ In Units	$U/\pi\rho$ In Units
1	16.00
2	14.67
3	11.56
4	8.67
5	6.93

In order to bring the potential to zero throughout the metal sphere it is only necessary to place the metal sphere in the hole of the cloud and add to the metal sphere a negative charge of magnitude such as to produce a potential

equal to but opposite in sign to the potential of the hole. We know that the potential of a conducting sphere is constant throughout and an examination of the hole in the cloud shows that it too has constant potential throughout.

The charge Q on a metal sphere to produce the potential necessary to cancel the potential of the hole is given by $Q = V\,C$, where V is potential, and C is the capacitance of the sphere. The capacitance of a conducting sphere is numerically equal to the radius, and thus we find that the Q on the sphere must be the negative voltage of the hole times the radius a or $Q = 2\pi\rho(b^2 - a^2)a$.

The potential V to depress the potential of hole to zero is given as follows

$$-V = Q/C = Q/a = -2\pi\rho(b^2 - a^2)a/a$$
$$= -2\pi\rho(b^2 - a^2) \ldots\ldots \rho \leq a \qquad (8)$$

$$-V = Q/\rho = -2\pi\rho(b^2 - a^2)a/\rho \ldots\ldots\ldots \rho \geq a \qquad (9)$$

The addition of the charged sphere to the hollow cloud is shown graphically in Figure (5b), page 20, and the values for $U/\pi\rho$ are given in Table III on the following page.

TABLE III

POTENTIAL OF HOLLOW CLOUD
WITH GROUNDED METAL SPHERE INSIDE
VS DISTANCE FROM THE CENTER

ρ In Units	U_{a+b} + (-V) In Units
1	0
2	6.67
3	6.23
4	4.67
5	4.00

The above addition shows a zero potential throughout the small sphere, a maximum potential about two-thirds of thickness of the cloud outward from the metal sphere and then a gradual dropping off until it reaches zero potential at infinity.

This type is approximated when a blanket of charged dust is laid down over a field by an airplane. The potential will be zero at the ground or plant surfaces, reach a maximum somewhere within cloud and again approach zero somewhere out in space.

The other case of interest is that of a cloud with boundaries of known controllable boundary values. We may take as an example a spherical cloud with a metal sphere in it, but this time with the outer boundary of the cloud at zero as well as the metal sphere at zero. The method used will be essentially the same as before, namely, the addition of several

simple charge distributions.

We may now start with the hollow cloud previously developed and add a negative charge at the outer boundary (a metal shell) until the potential of the shell is reduced to zero. The effect on the inside of the cloud due to this negative charge is a constant reduction of potential all over the cloud. This is shown in Figure (6b), page 21.

The value of the constant to be subtracted is given by

$$(U_{a+b})_{\rho=b} = 4\pi\sigma(b^3 - a^3)/3b \qquad (10)$$

The potential of the distribution is equal to

$$U_{a+b} - (U_{a+b})_{\rho=b} \quad \ldots\ldots\ldots\ldots\ldots\ldots\ldots\ldots 0 \leq \rho \leq b \qquad (11)$$

$$U_{a+b} - (U_{a+b})_{\rho=b} = 2\pi\sigma(b^2 - a^2) - 4\pi\sigma(b^3 - a^3)/3b \ldots\ldots\ldots\ldots \rho \leq a \qquad (12)$$

$$U_{a+b} - (U_{a+b})_{\rho=b} = -2\pi\sigma\rho^2/3 + 2\pi\sigma b^2 - 4\pi\sigma a^3/3\rho - 4\pi\sigma(b^3 - a^3)/3b \ldots\ldots\ldots a \leq \rho \leq b \qquad (13)$$

$$U_{a+b} - (U_{a+b})_{\rho=b} = 0 \ldots\ldots\ldots\ldots\ldots\ldots\ldots\ldots \rho \geq b \qquad (14)$$

Table IV gives the values of $U_{a+b} - (U_{a+b})_{\rho=b}/\pi\sigma$ from $0 \leq \rho \leq 5$, where $a = 1$, $b = 3$.

TABLE IV

POTENTIAL OF A HOLLOW CLOUD WITH THE OUTER BOUNDARY AT ZERO VS DISTANCE FROM THE CENTER

ρ In Units	$U_{a+b} - (U_{a+b})_{\rho=b} / \pi\phi$ In Units
1	4.44
2	3.11
3	0
4	0
5	0

The final case of interest is that of a hollow cloud containing both a metal sphere at zero potential and the boundary at zero potential. This is shown in Figure (7b), page 21, and can be calculated for the general case as follows: The potential of a hollow cloud is added to the potentials due to the negative charges on a grounded sphere and a grounded metal shell. The value of the negative charges on the sphere and the shell can be, but need not be found. It is just as easy to find the value of the depressing potential necessary to bring the metal sphere and metal shell to zero simultaneously. The following formula gives this potential throughout the cloud.

$$0 = U_{a+b} - (U_{a+b})_{\rho=b} - V\,(1 - a/b) \ldots\ldots \rho = a \qquad (15)$$

At $\rho = a$ the potential = 0 by definition.

We have taken the hollow cloud at zero potential on the outside boundary and added an amount aV/b to it to compensate for the negative value of the depressing potential $-V$ at $\rho = b$ from the consideration that Q (the charge on the metal sphere) $= VC = Va$, where $C = a$ is the capacitance of the metal sphere.

$$V = \frac{U_{a+b} - (U_{a+b})_{\rho=b}}{(1 - a/b)}$$

$$V = \frac{-2\pi\rho\rho^2/3 + 2\pi\rho b^2 - 4\pi\rho a^3/3\rho + 4\pi\rho(a^3 - b^3)/3b}{(1 - a/b)} \qquad (16)$$

If $V' = V/\pi\rho$, then for $a = 1$, $b = 3$

$$V' = \frac{-2/3 + 18 - 4/3 - 4\,(27 - 1)/9}{1 - .333} = \frac{4.44}{.667} = 6.66 \qquad (17)$$

Throughout the metal sphere the depressing voltage $= V$, but since potential at a distance from the charged sphere due to the charge $Q = VC = Va$ is given by the relation $Q/\rho = Va/\rho$, then at $\rho = b$ the depressing potential $= aV/b$. In order to get the potential distribution throughout the cloud we now must subtract the depressing potential from, and add the constant aV/b to the potential of the hollow cloud whose outer boundary was at ground potential.

$$U = U_{a+b} - (U_{a+b})_{\rho=b} - V/\rho + aV/b$$

$$U = -2\pi\rho\rho^2/3 + 2\pi\rho b^2 - 4\pi\rho a^3/3\rho + 4\pi\rho(a^3 - b^3)/3b - V/\rho + aV/b \qquad (18)$$

$$U/\pi\rho = -2\rho^2/3 + 2b^2 - 4a^3/3\rho + 4(a^3 - b^3)/3b - V'/\rho + aV'/b \qquad (19)$$

For $a = 1$, $b = 3$, $V' = 6.66$

$$U/\pi\rho = -.667\rho^2 + 18 - 1.33/\rho - 11.56 - 6.66/\rho + 2.22 \quad \text{.....} \quad a \leq \rho \leq b \qquad (19)$$

$$U/\pi\rho = 0 \text{ for } 0 \leq \rho \leq a \text{ and for } \rho \geq b \qquad (20)$$

Table V gives the values of $U/\pi\rho$ for $0 \leq \rho \leq 5$. Figure (7b), page 21, shows the potential distribution of this case.

TABLE V

POTENTIAL OF A HOLLOW CLOUD HAVING A METAL SPHERE WITHIN AT ZERO POTENTIAL AND AN OUTER BOUNDARY AT ZERO POTENTIAL VS THE DISTANCE FROM THE CENTER

ρ In Units	$U/\pi\rho$ In Units
1	0
1.5	1.83
2.0	2.00
2.5	1.30
3	0
4	0
5	0

Superposition of Simple Electric Fields

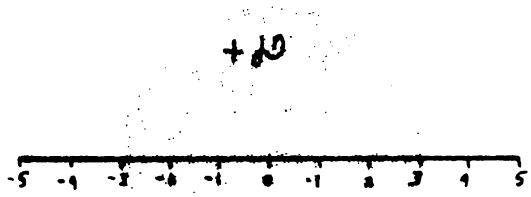

Fig. 1a. Cross-section of large positive cloud.

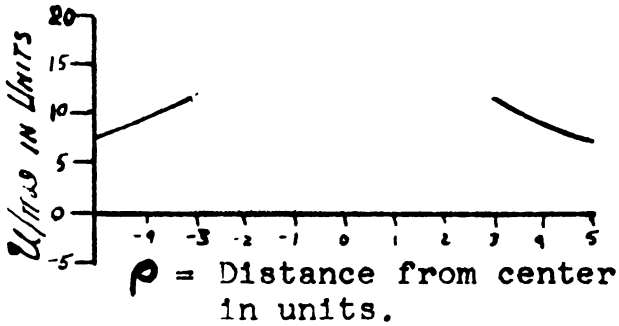

Fig. 1b. Potential along horizontal diameter of cloud.

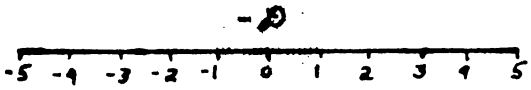

Fig. 2a. Small negative cloud.

Fig. 2b. Potential distribution along a horizontal diameter of negative cloud.

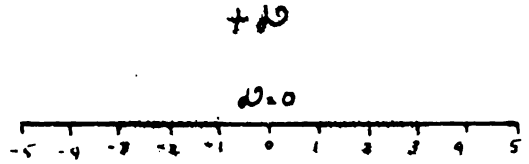

Fig. 3a. Cross-section of hollow cloud.

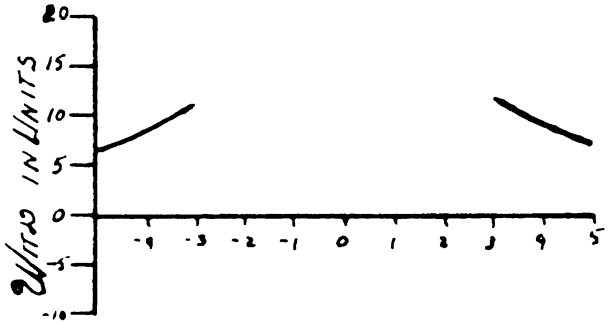

Fig. 3b. Potential distribution of hollow cloud.

Superposition of Simple Electric Fields

Fig. 4a. Cross-section of metal sphere.

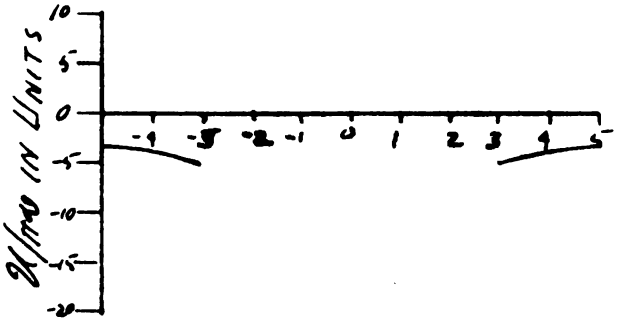

Fig. 4b. Potential distribution of negatively charged sphere.

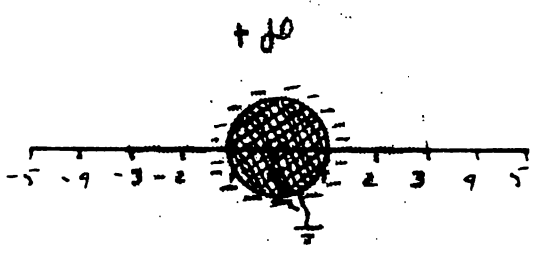

Fig. 5a. Cross-section of negatively charged sphere inside of hollow cloud.

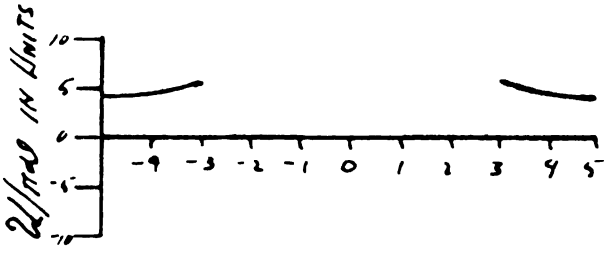

Fig. 5b. Potential distribution of the sum of negatively charged metal sphere and hollow cloud along extended horizontal diameter.

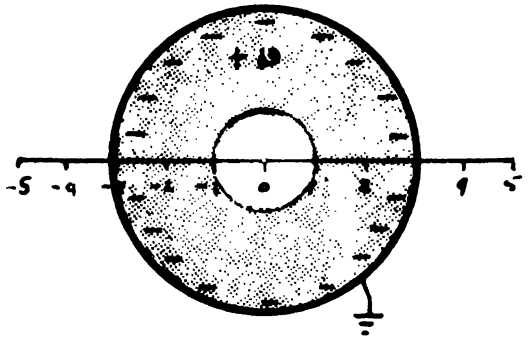

Fig. 6a. Cross-section of a hollow cloud enclosed by a conducting shell at zero potential.

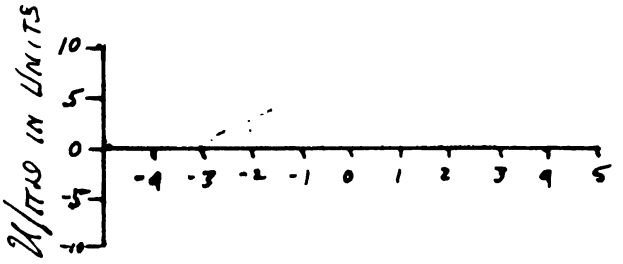

Fig. 6b. Potential distribution along extended horizontal diameter of hollow cloud with boundary of cloud earthed.

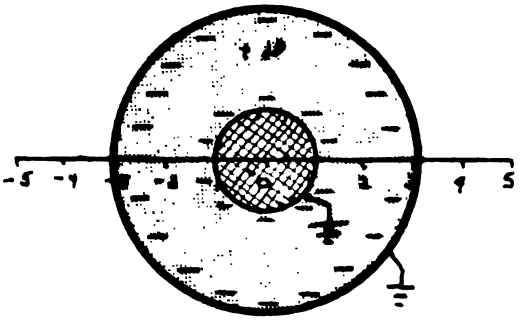

Fig. 7a. Cross-section of a metal sphere in a hollow cloud enclosed by a conducting shell at ground.

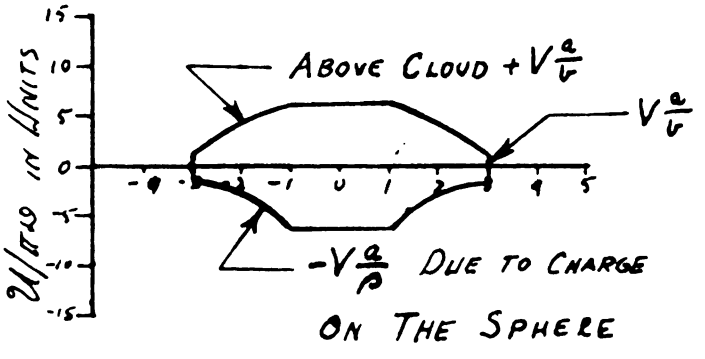

Fig. 7b. Potential distribution along an extended horizontal diameter of sum of potentials of grounded metal sphere, hollow cloud, and a grounded metal shell.

Calculations of Potential Distribution of a Spherical Cloud of Charged Dust That was Measured.

Since it is desirable to compare a measured field and calculated field, the calculated field must have the same boundaries and charge density ρ as the measured fields.

The charge density ρ is taken to be .645 units/cu. inch, which value is 1938 times the value of ρ' in e.s.u./cc.

If $Q = 4\pi R^3 \rho'/3$ for total charge contained in a spherical cloud of radius R and charge density ρ' then $V = Q/R = 4\pi R^3 \rho'/3R$ = potential at outer boundary of this cloud. Then $\rho' = 3V/4\pi R^2$. Considering that 1 stat volt = 300 volts and 1 cm. = .394 inches, we may convert from c.g.s. units to volts and inches by using the following factor

$$\frac{\rho'}{\rho} = \frac{\frac{1}{(4\pi\ 1^2)/3}}{\frac{300}{[4\pi(.394)^2]/3}} = \frac{1}{1938}$$

$$\rho'(1938) = \rho(1) \qquad (21)$$

The diameter of the cloud is 35.5 inches and the diameter of the metal sphere to be used inside it is .90 inches. In terms of the distance ρ from the center this means the outer boundary of cloud is (b = 17.75 inches) and the radius of the metal sphere is (a = .45 inches).

The calculation for Case I is that of a cloud with no metal sphere in it but depressed to zero potential at the

outer boundary. The equation as found by methods of the former section is as follows

$$U = 2\pi\sigma(b^2 - \rho^2)/3 \qquad (22)$$

with $\sigma = .645$, $b = 17.75$

$$U = 1.35\ (315 - \rho^2) \qquad (22)$$

The following table gives the values of the potential for the various positions as calculated from the above formula to the nearest volt.

TABLE VI

CALCULATED POTENTIAL VS
DISTANCE FROM CENTER FOR CASE I

ρ Inches from Center	ρ^2	$(b^2 - \rho^2)$ $(315 - \rho^2)$	U $1.35\ (b^2 - \rho^2)$ volts
.45	.202	315	425
2.25	5.06	310	418
4.25	18.1	297	401
6.25	39.1	276	373
8.25	68.	247	333
10.25	105.	210	284
12.25	150.	165	222
14.25	203.	112	151
16.25	267.	48	65
17.75	315.	0	0

For Case II, where the metal sphere is depressed to 200 volts and the outer boundary is at zero, the equation for the cloud depressed to zero potential at the outer boundary is given from a previous section as

$$U = 2\pi\rho_0(b^2 - \rho^2)/3 - 4\pi\rho_0 a^3/3\rho + 4\pi\rho_0 a^3/3b \ldots\ldots\ldots a \leq \rho \leq b \qquad (13a)$$

$$U = 1.35\,(315 - \rho^2) - .246/\rho + .246/17.75 \ldots a \leq \rho \leq b$$

It can be seen that the second term on right can never be greater than .550 nor less than .013. The third term on right side of equation equals .013. Thus the maximum error that can result from neglecting these two terms is .550 - .013 = .537 volt. This is an entirely negligible value when considering the magnitude of the first term on right side of equation having a maximum value of 425 volts. The second and third terms will be dropped from all subsequent calculations. The equation of hollow cloud is now given as

$$U = 1.35\,(315 - \rho^2) \ldots\ldots\ldots\ldots a \leq \rho \leq b \qquad (13b)$$

The equation of hollow cloud with metal sphere at 200 volts and outer boundary at zero potential is given by

$$U = 2\pi\rho_0(b^2 - \rho^2)/3 - aV/\rho + aV/b \qquad (23)$$

V being the depressing potential and found by method of previous section as follows

$$U = 200 = 1.35\ (315 - .2) - V\ (1 - a/b) \ldots\ldots \rho = a \qquad (24)$$

$$V = 231 \text{ volts}$$

$$aV/b = 6 \text{ volts}$$

$$U = 1.35\ (315 - \rho^2) - .45\ (231)/\rho + 6 \text{ volts} \ldots a \leq \rho \leq b \qquad (23a)$$

TABLE VII

CALCULATED POTENTIAL VS
DISTANCE FROM CENTER FOR CASE II

ρ	$2\pi\omega(b^2 - \rho^2)/3$	aV/ρ	aV/b	U
Inches from center	$1.35\ (315 - \rho^2)$	$- .45\ (281)/\rho$	+ 6	volts
.45	425	231		+ 200
2.25	418	46		378
4.25	401	24		383
6.25	373	17		362
8.25	333	13		326
10.25	284	10		280
12.25	222	8.5		220
14.25	151	7.3		150
16.25	65	6.4		65
17.75	0	5.9		0

For Case III where the metal sphere is at ground, a negative charge is induced on the sphere sufficient to depress the original 425 volts down to zero at the surface of the metal sphere. The procedure for calculation is exactly the

same as in the preceding case and a value for the depressing voltage V must be obtained.

$$U = 0 = 2\pi\rho(b^2 - a^2)/3 - aV/a + aV/b \ldots . \rho = a$$
$$0 = 425 - V(1 - a/b) \qquad (24)$$

$V = 436$ volts

$aV/b = 11$ volts

$$U = 1.35(315 - \rho^2) - .45(436)/\rho + 11 \text{ volts} \ldots . a \leq \rho \leq b \qquad (25)$$

TABLE VIII

CALCULATED POTENTIAL VS
DISTANCE FROM CENTER FOR CASE III

ρ	$2\pi\rho(b^2 - \rho^2)/3$	aV/ρ	aV/b	U
Inches from center	$1.35(315 - \rho^2)$	$-.45(436)/\rho$	+ 11	volts
.45	425	436		0
2.25	418	87		342
4.25	401	46		366
6.25	373	31		353
8.25	333	24		320
10.25	284	19		276
12.25	222	16		217
14.25	151	14		148
16.25	65	12		64
17.75	0	11		0

Case IV has the metal sphere depressed to a negative 198 volts, and is handled exactly the same fashion. Solving for V we have.

$V = 639$ volts

$aV/b = 16$ volts

$$U = 1.35\ (315 - \rho^2) - .45\ (639)/\rho + 16 \text{ volts} \ldots a \leq \rho \leq b \quad (26)$$

TABLE IX

CALCULATED POTENTIAL VS
DISTANCE FROM CENTER FOR CASE IV

ρ	$2\pi\rho\sigma(b^2 - \rho^2)/3$	aV/ρ	aV/b	U
Inches from center	$1.35\ (315 - \rho^2)$	$- .45\ (639)/\rho$	+ 16	volts
.45	425	639		- 198
2.25	418	130		+ 304
4.25	401	69		+ 348
6.25	373	47		+ 342
8.25	333	35		+ 314
10.25	284	28		+ 272
12.25	222	24		+ 214
14.25	151	20		+ 147
16.25	65	18		+ 63
17.75	0	16		0

Measured Potential Distribution of a Spherical Cloud of Charged Dust

The first real attempt to measure the potential distribution (from which the field intensity could be deduced) was a complete failure. A closed pyrex spherical container was filled with a cloud of charged smoke, by evacuating the container partially so that the smoke was drawn through an ionized field type charging nozzle. The filling apparatus was all mounted in a tight fitting stopper. Once the flask was filled with charged smoke, the stopper with the filling apparatus was replaced by another stopper containing a movable radioactive probe connected to an electrostatic voltmeter. However, it was found that the time required to replace the filling stopper with the measuring stopper and bring the instrument up to potential was sufficient that an essentially constant potential occurred throughout the volume of the flask. This could only mean that the smoke particles had almost all precipitated onto the inside of the flask. Nothing whatever was learned of the potential distribution that would occur in a uniformly charged cloud. This apparatus is shown in Figures (8) and (9).

The second attempt utilized a continuous cloud of charged dust which was not so greatly affected by precipitation. The continuous cloud of dust was made available to the volume region being measured to replenish the dust that precipitated out of the air. Also, conducting surfaces held at known

potentials were used as boundaries to the cloud instead of insulated boundaries that changed potential with a precipitation of dust and charge. These conducting boundaries dissipated the charge brought to the boundaries by the precipitated dust so there was no appreciable effect due to dust precipitation such as occurred in the first attempt.

The apparatus to provide the charged dust and the measuring system are pictured in Figure (10) and (11), and a schematic diagram is shown in Figure (12).

Description of Apparatus.

The apparatus for producing a charged dust cloud and delivering it to the measuring region consisted of the following items: A variable speed motor operating a centrifugal fan for producing a dust cloud, an ionized field type charging nozzle mounted on the end of fan discharge pipe for charging the dust, a power supply for supplying power to the charging needle, a mixing chamber into which the dust was blown and mixed with air, a measuring chamber, a perforated bulkhead between mixing chamber and measuring chamber to provide a reasonably uniform discharge of charged dust into measuring chamber, an exhaust fan to draw the dust from mixing chamber into measuring chamber, and an axial flow fan to provide turbulence in the measuring chamber.

Apparently due to the location of the exhaust outlet in the top of the rear end of the measuring chamber, the dust

cloud was prone to move in such manner as to allow a greater concentration of charge (and presumably dust, although this could not be visibly detected) nearer the upper part of the measuring chamber. This condition resulted in a somewhat lop-sided potential distribution. This condition was greatly improved by the use of an axial flow fan placed as shown in the diagram of Figure (12). The fan improved the distribution no matter whether directed along the floor, toward center of cage or toward ceiling, but gave best results when positioned along floor of measuring chamber as shown.

The apparatus for measuring the potential of the charged cloud consisted of a chicken wire spherical cage of 35.5 inches diameter (which formed a cloud with a spherical shape when the cage was placed at zero potential), a reference probe and electroscope type voltmeter, a movable probe (traverse probe) and electrostatic voltmeter, a cord and pulley arrangement for supporting the movable probe, and an indexed pulley for taking up or letting out cord which raised or lowered the traverse probe.

Other equipment included a sling psychrometer for measuring the wet and dry bulb temperatures.

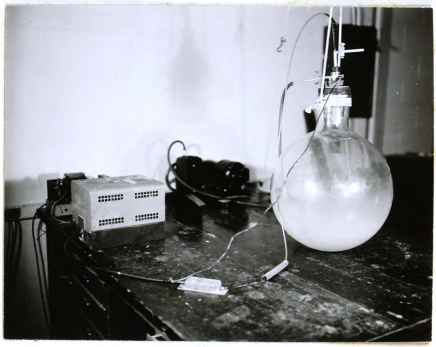

Fig. 8. Spherical flask with filling cap and charging apparatus in position.

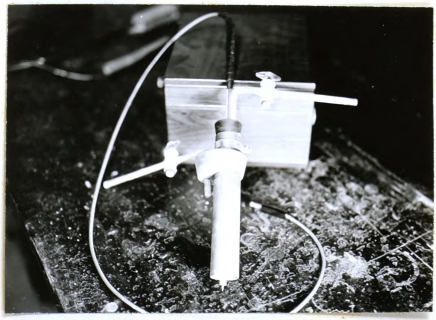

Fig. 9. Charging nozzle and filling cocks as used in Figure 8.

Fig. 10. View of apparatus used for measuring potential distributions along a vertical diameter of a charged dust cloud.

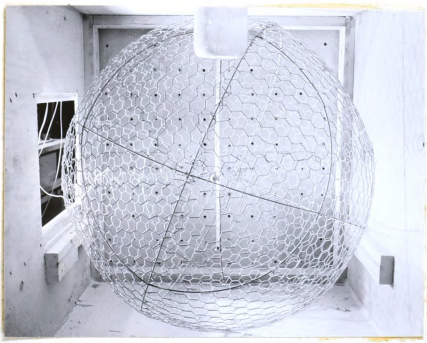

Fig. 11. View of measuring chamber showing spherical cage, reference probe (black lead), traverse probe (glass rod insulated), and metal sphere. In the background can be seen perforated bulkhead.

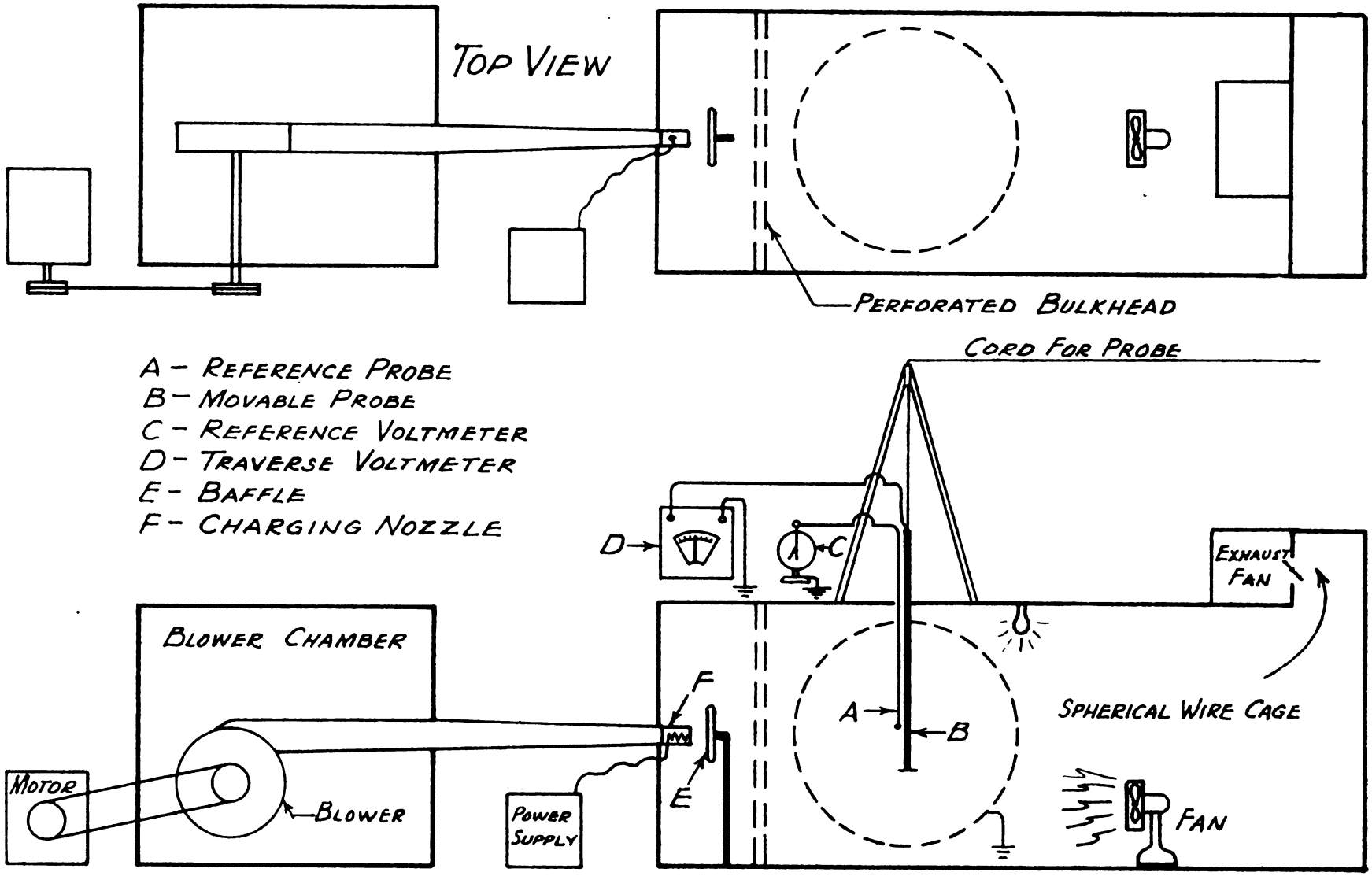

Fig. 12. Diagram of apparatus for measuring potential distribution in a charged dust cloud.

Procedure for Making a Potential Traverse along a Vertical Diameter of a Charged Dust Cloud.

The adjustable gate on the exhaust fan outlet was nearly closed. This reduced the pulse effect due to the uneven feeding of dust to the blower. An axial flow fan (of household type) was operated to promote a mixing of dust and charge within the measuring chamber. The centrifugal blower was operated at 1500 r.p.m. for all traverse measurements. The charging nozzle was supplied with an ionizing voltage (approximately + 13000 volts D.C.). The dust (325 mesh attaclay) was fed into the centrifugal blower by hand in discrete quantities of somewhat less than a gram by shaking through a sieve (similar to a small flour sifter). After an initial filling of the measuring chamber only one addition of dust was required for a reading.

The reference probe was taped in place at one of the measuring stations and the reference dots on the glass faces of the meter were lined up at a voltage that would allow near full scale deflection on the traverse meter when at the station of maximum potential. The potentials on the metal sphere dictated to a large extent where the reference probe could be placed. The reference meter was operated in the range of 215 volts to 425 volts depending on the particular case being measured. The traverse probe had a three foot glass tube for an insulator at the measuring end, which was sufficiently

heavy to keep the supporting cord under tension at all times. An indexed pulley (Figure 10) was calibrated so that by turning the pulley to a given mark, the probe was raised or lowered to one of the observations stations. The station positions were measured in two inch increments from the top of the spherical cage for convenience in calibration. This led to some inconvenience in all subsequent operations with the data since the sphere was only 35.5 inches in diameter. The cotton cord stretched the first couple of days but was recalibrated for each test, and checked after each test to be sure no change had taken place. After two or three days the cord did not stretch any observable amount.

Three replications of readings were taken for each station. The order of observation of each reading for all stations was determined by a complete randomization of the total readings to be taken. Thus the first reading of station one might be followed by the first reading of station twelve. Since the complete traverse required 51 observations not counting the two end points on the grounded cage, the last reading of some of the stations was taken as long as an hour and a half after the first reading. This randomization was considered necessary in order to confound any gradual changes in the measuring system due to changes in relative humidity, or other variables unknown to the experimenter over the two hour duration of the test.

The reference probe was located in one position throughout test and the position checked by means of the traverse

probe several times during the test. Once the reference meter was calibrated for a traverse, all readings on the traverse meter were taken at the moment the tip of the gold leaf of the reference meter fell past the bottom of the index dots on the meter faces. A falling leaf on reference meter and falling needle on traverse meter was used for all observation of readings. This was done to insure that the bending stress in the gold leaf was always in the same direction. Characteristic of a radioactive probe such as was used for both reference and traverse probes is that it approaches the surrounding potential asymptotically and, therefore, there is necessarily a small amount of lag with the falling leaf. This means that a falling leaf or needle would read somewhat higher than the true potential and a rising leaf or needle somewhat less than the true potential. However, indications were that this lag was not of nearly as large magnitude as discrepancies that would arise due to variable bending stress in the gold leaf. The voltage difference on the same point for a falling as compared to rising leaf was somewhere in the neighborhood of fifteen volts, which variation could be expected among different readings of the same point if no consideration were given to method of approach to the point. On the other hand, replications of a given reading using fast falling, slow falling and steady held readings approached from top down did not show any observable differences in value of potential other than could be attributed to less

accurate observing and announcing of arrival at point by the reference meter observer. A hovering leaf is harder to detect when it is at an exact position than is a moderately falling leaf. A fast falling leaf is often not called correctly because of inaccurate anticipation of the observer and inaccurate announcement of arrival. For example, an inaccurate announcement of one-tenth of a second on a fast falling leaf of perhaps 30 volts per second would amount to 3 volts error. Also a fast falling needle on traverse meter is subject to the same type of error which may add another two or three volts to the error. For this reason, a slowly falling leaf of five to ten volts per second gave the most consistent results. Repeated observations of a given point would usually be within two or three volts and often four or five readings could be taken in rapid succession that were within one volt of each other. The technique described requires some practice for consistency and naturally is subject to some errors, however, even unpracticed observers are able to read to within one or two volts of the reading of experienced observers.

There were four potential traverses carried out tracing the potential distributions due to four different boundary conditions placed on a spherical dust cloud of approximately uniform charge density. In all cases the outer boundary of the cloud (formed by a chicken wire cage) was held at zero potential. In the first case the traverse was of the potential of a vertical diameter of the cloud without a metal sphere in

it. The second case was of approximately the same cloud with a metal sphere of diameter .9 inches centered in it having a potential of + 200 volts impressed upon it. The third case was for a metal sphere centered in approximately the same dust cloud with zero potential impressed upon it. The fourth case was for approximately the same cloud with a - 198 volts impressed upon the sphere. In the second and fourth cases the potential on the sphere was obtained by connecting the metal sphere to a 200 volt battery hook-up. In the third case the metal sphere was connected to ground. The lead of the metal sphere was inside of an 8,000 volt break down strength spaghetti tubing.

The whole traverse from top of sphere to bottom was carried out several times in preliminary traverses and also for the Case I. However, it was decided that since the two halves of the diameter from top to center, and bottom to center were quite similar (though not exactly so) it would be expedient to carry out only the bottom half of the traverse (from bottom to center). This decision came about because the test was shortened from two hours to one hour and thus would reduce variations due to changes in relative humidity, temperature and fatigue of operators. The bottom half was chosen because it most closely followed the theoretical calculations for Case I.

The data for all four cases are given in Tables X, XI, XII and XIII. Discussion as to the results of the tests will

be reserved until a later chapter where the traverses are compared with the calculated traverses of the previous chapter.

The original data reckoned the stations of observation as taken in two inch increments from the top of the sphere. However, in the data presented the positions of observation are given in inches from the center to correspond to the formulae for the calculated traverses which gives the potential as a function of the distance from the center.

Case I represents the condition of a homogeneous cloud of charged dust with the outer boundary at zero potential. The data given in Table X are for the potentials existing along a vertical radius.

TABLE X

MEASURED POTENTIAL VS DISTANCE FROM CENTER FOR CASE I

Inches from center	Potential in Volts			
	Rep. 1	Rep. 2	Rep.3	Ave.
0	403	402	403	403
2.25	393	393	394	393
4.25	371	367	373	370
6.25	340	341	350	344
8.25	310	306	316	311
10.25	258	256	257	257
12.25	215	220	214	216
14.25	163	150	153	155
16.25	75 - 85	70 - 80	70 - 80	75
17.75	0	0	0	0

Case II represents the conditions where the potential on a metal sphere at the center of the cloud is approximately half way between zero and the potential it would assume if isolated. The potential was held on the sphere by means of a 200 volt battery hook up. The reference probe was placed at 12.25 inches from the center of the cloud and calibrated so that it read 216 volts at that position. This was done because it was desired to have comparative densities for all cases, and it was noted that theoretically for all four cases the potential of the curves were close to a common value at any of the positions close to the outer boundary of the cloud. The data for Case II are given in Table XI.

TABLE XI

MEASURED POTENTIAL VS DISTANCE FROM CENTER FOR CASE II

Inches from center	Potential in Volts							
	Rep. 1	Rep. 2	Rep. 3	Rep. 4	Rep. 5	Rep. 6		Ave.
.45	+ 200	+ 200	+ 200					+ 200
2.25	356	375	374	386	385	384	385*	380
4.25	378	372	370	375	373	373		373
6.25	338	343	346					342
8.25	300	303	306					303
10.25	250	246	248					248
12.25	223	216	215				214*	218
14.25	160	159	153					157
16.25	70 - 80	70 - 80	70 - 80					75
17.75	0	0	0					0

* These two readings taken after the other readings to ascertain whether or not the circled group was higher than previous readings as station because of a change in reference voltage.

Case III represents the conditions where both the metal sphere and the outer boundary are at zero potential. The data for Case III are given in Table XII.

TABLE XII

MEASURED POTENTIAL VS DISTANCE FROM CENTER FOR CASE III

Inches from center	Potential in Volts			
	Rep. 1	Rep. 2	Rep. 3	Ave.
.45	0	0	0	0
2.25	346	350	346	347
4.25	372	373	372	372
6.25	343	338	340	340
8.25	298	300	295	298
10.25	250	246	253	250
12.25	213	217	220	217
14.25	155	160	165	160
16.25	70 - 80	70 - 80	70 - 80	75
17.75	0	0	0	0

Case IV represents the conditions where a potential of a negative 198 volts is on the metal sphere and all other conditions remain the same. The values of potentials at various distances from the center are given in Table XIII.

TABLE XIII

MEASURED POTENTIAL VS DISTANCE FROM CENTER FOR CASE IV

Inches from center	Potential in Volts						
	Rep. 1	Rep. 2	Rep. 3	Rep. 4	Rep. 5	Rep. 6	Ave.
.45	- 198	- 198	- 198				- 198
2.25	+ 296	+ 300	+ 313	+ 300	+ 310	+ 305	+ 304
4.25	333	330	328				+ 330
6.25	329	326	320				+ 325
8.25	245	298	298	295	298	293	+ 297
10.25	243	255	253	251	255	253	+ 253
12.25	218	223	215				+ 219
14.25	162	175	165				+ 167
16.25	70 - 80	70 - 80	70 - 80				+ 75
17.75	0	0	0				0

* The thirty readings included in the first three replications of Table XIII were completely randomized as to order in which reading was taken.

At those positions where some one value differed from the average of the closest two by more than ten volts, three more replications were made, one after the other at the end of the test. When only three replications were used the mean of the three was taken for an average. When six replications were used, the highest and lowest were discarded and the mean of the other four was used as an average.

Comparison of Calculated and Measured Potential Distributions

The purpose of obtaining both measured and calculated potential distributions was to verify the correctness of the calculated method by means of a comparison of the similarity of calculated and measured curves.

There are only two details by which we can judge the similarity. They are (1) the correspondence of the general shape of each case between measured and calculated and (2) the order of ascendency of the curves of the four cases.

The measured potential distribution has been adjusted in those cases where necessary to correspond to the calculated potential at the position of the reference probe using a charge density ρ of .645 units/cu. inch. This meant multiplying the potentials except at boundaries for Case I by a factor 1.03, Case II by 1.01, Case III by 1.00, and Case IV by 0.978.

It is recognized that there is some danger in making an adjustment of this kind because the standard deviation of this point is quite large being 3.18 volts for Case I, 4.36 volts for Case II, 4.96 volts for Case III and 4.05 volts for Case IV. However, under the circumstances some sort of adjustment had to be made and all cases were treated in like fashion.

It will be noted that the calculated potential is higher in the range 6 12 than the measured, but becomes less

than the measured potential for the range $13 < \rho < 17.75$ for all four cases. This indicates that there is a low density of charge in the region $6 < \rho < 12$ and a high density of charge in $13 < \rho < 17.75$. The high and low density are with respect to μ = .645 units/cu. inch. There are two possible causes of this slight inhomogeneity, (1) the dust cloud produced in the chamber was not uniform regardless of whether the dust was charged or not, and (2) the electric field forces set up by the charged dust cloud tended to gravitate dust nearer the conducting surfaces at the expense of the inner regions of the cloud. There is some indication, though not conclusive, that this was taking place both near the sphere and near the outside boundary. Probably both of the above factors contribute to the condition.

There is little doubt as to the similarity of shape of measured and of calculated potential distribution curves for each of the cases, as may be noted by observing Figures (13), (14), (15) and (16) which compare measured and calculated potentials for Cases I, II, III and IV respectively. The Case IV, Figure (16), deviates the greatest amount, but there can be no mistaking the similarity of the general shape of Case IV for it is quite distinct from any of the other cases.

The order of ascension of the curves starting with Case IV and going up is the same for both calculated and measured as can be seen by comparing Figures (17) and (18).

TABLE XIV

SUMMARY OF POTENTIALS FOR MEASURED AND CALCULATED
POTENTIAL DISTRIBUTION OF A SPHERICAL CLOUD OF CHARGED DUST

ρ	Case I			Case II			Case III			Case IV		
Inches from center	A	B	C	A	B	C	A	B	C	A	B	C
0	403	414	425	200	200	200	0	0	0	- 198	- 198	- 198
.45	---	---	---	200	200	200	0	0	0	- 198	- 198	- 198
2.25	393	403	418	380	383	378	347	347	342	+ 304	+ 297	+ 304
4.25	370	380	401	373	376	383	372	372	366	330	322	348
6.25	344	353	373	342	345	362	342	342	353	325	317	342
8.25	311	319	333	303	306	326	298	298	320	297	290	314
10.25	257	264	284	248	250	280	250	250	276	253	247	272
12.25	216	222	222	218	220	220	217	217	217	219	214	214
14.25	155	159	151	157	158	150	160	160	148	167	163	147
16.25	75	77	65	75	76	65	75	75	64	75	73	63
17.75	0	0	0	0	0	0	0	0	0	0	0	0

A - Measured potential average.
B - Adjusted average of measured potential to approximate the same ρ throughout the group.
C - Calculated potential with ρ = .645 units/cu. inch.

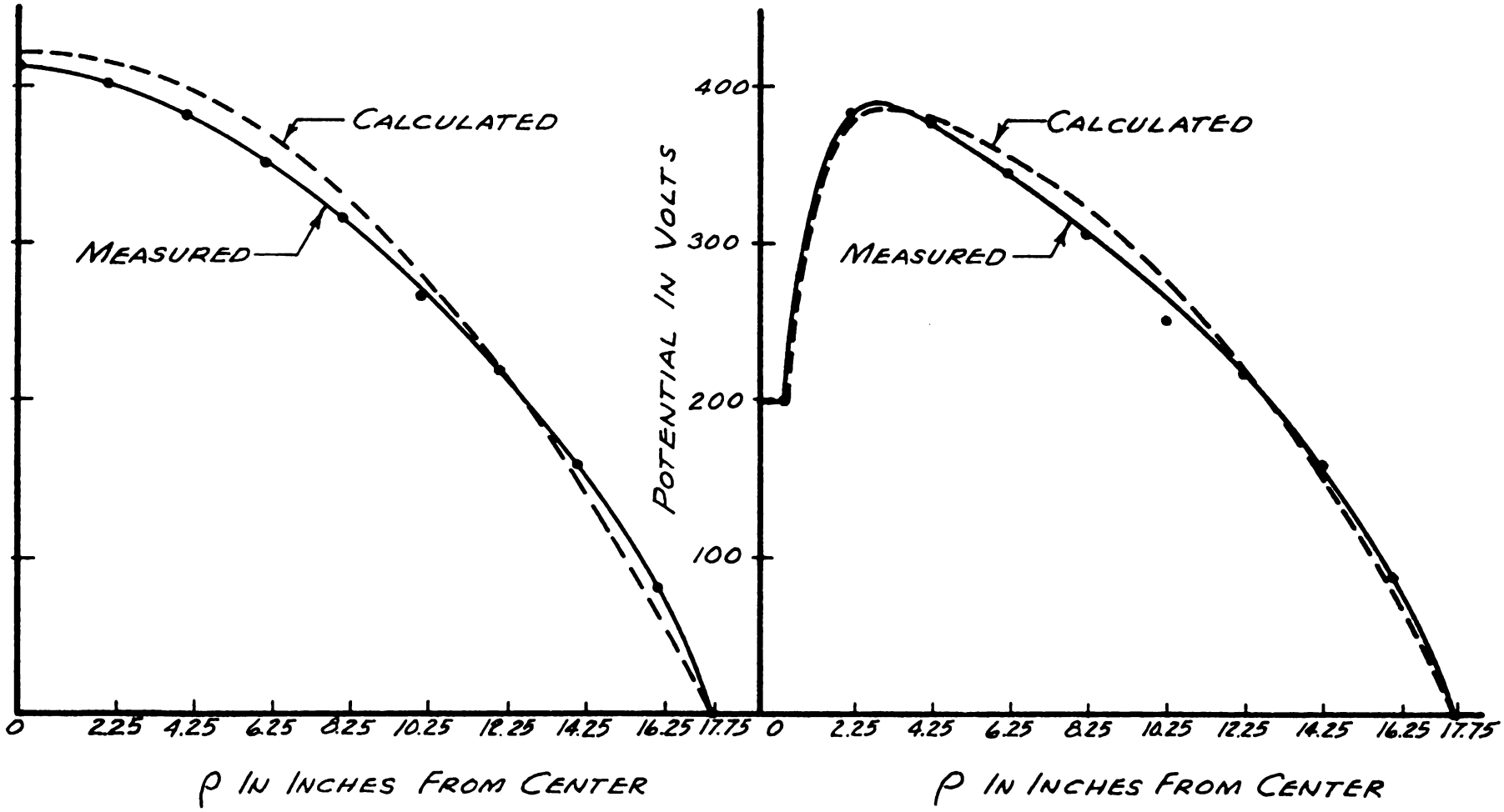

Fig. 13. Comparison of potential distribution for Case I, Measured versus calculated.

Fig. 14. Comparison of potential distribution for Case II, Measured versus calculated.

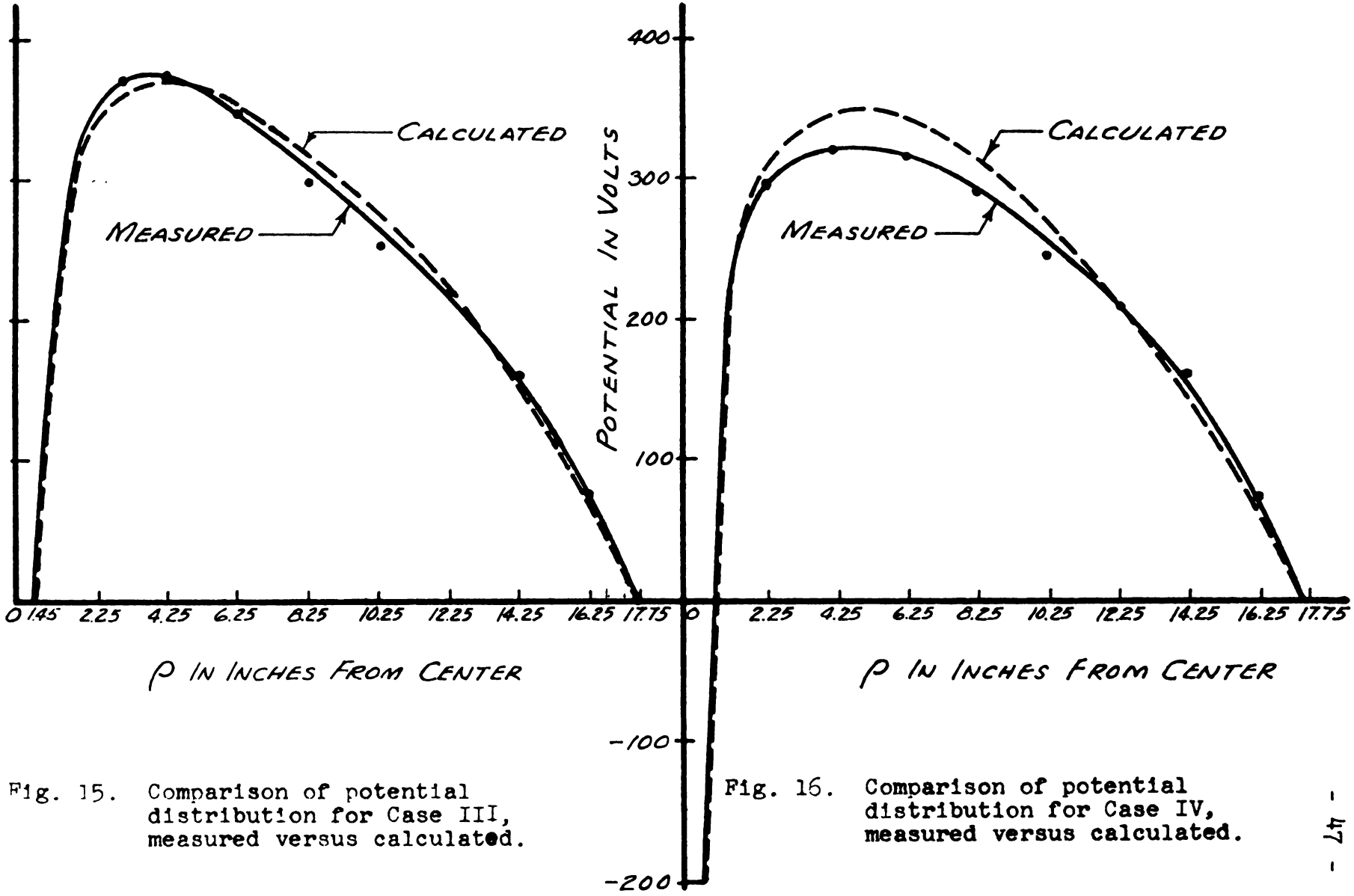

Fig. 15. Comparison of potential distribution for Case III, measured versus calculated.

Fig. 16. Comparison of potential distribution for Case IV, measured versus calculated.

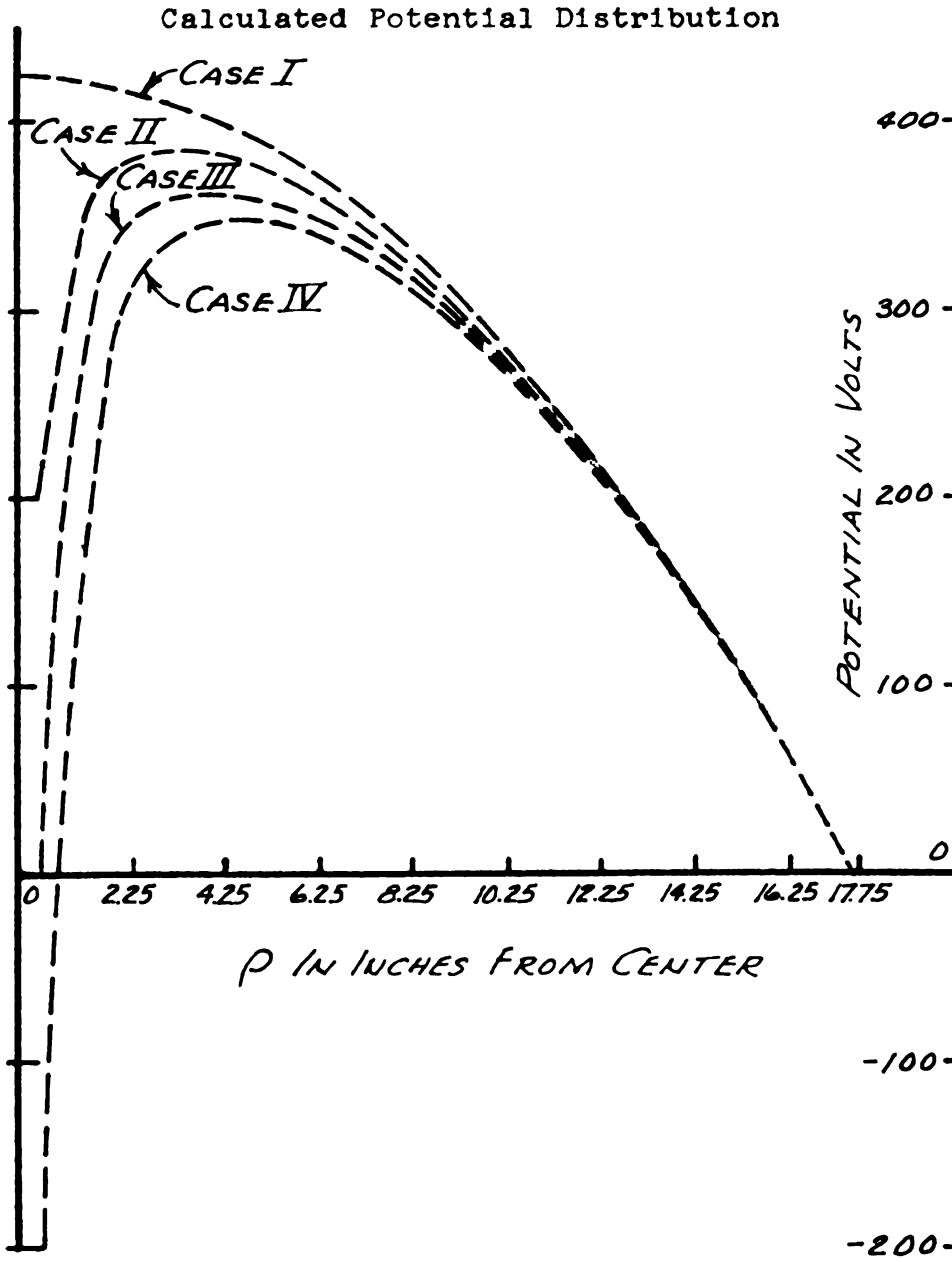

Fig. 17. Calculated potential distribution for Cases I, II, III and IV. ρ = .645 units/cu inch.

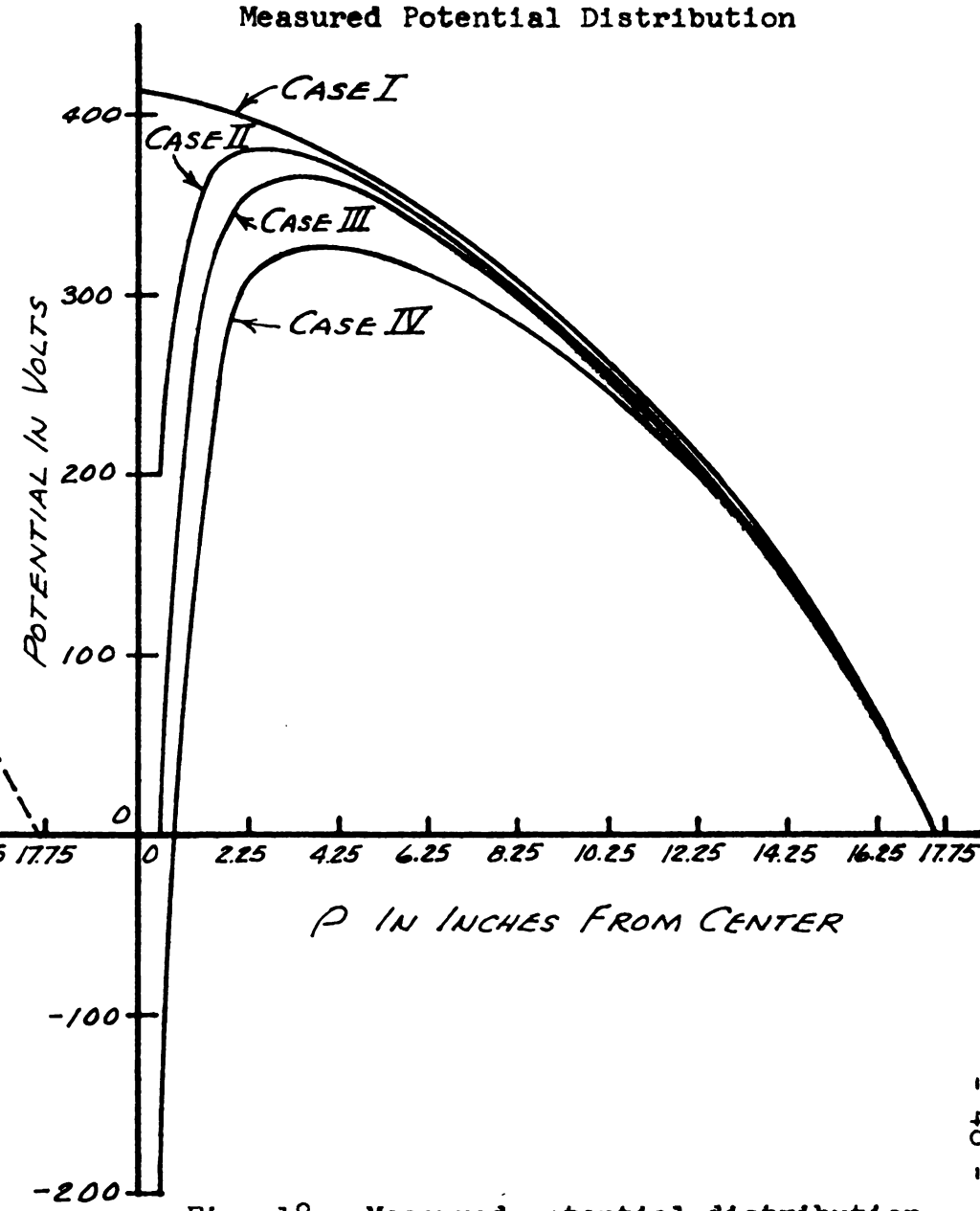

Fig. 18. Measured potential distribution for Cases I, II, III and IV. ρ = .645 units/cu inch.

With the aforementioned considerations there does not appear to be any major difficulty in accepting the results of the comparison as indicating the validity of the calculation. The author is going to base all further discussion of deposition theory and potential concepts on the supposition that the calculations have been verified and the method of superposition may be applied to the other particular electric fields as are of interest to electrostatic dusting techniques.

Present Concept of Dust Deposition

The electrostatic force on a dust particle carrying a charge Q is a product of the charge and the electrical field intensity E, thus the force is $F = EQ$. The field intensity is the negative of the potential gradient. The negative comes about because like signs repel for electrical charges.

In the potential distribution of Case IV, Figure (17), it will be noted that the gradient is zero throughout the metal sphere, is very steep in the regions of the cloud near the sphere and extending an inch or so out into the cloud, but gradually becoming less steep as we progress outward until it actually becomes horizontal at the top of the potential curve. This is some four and a quarter inches out into the cloud. A charged particle being of the population of the cloud producing the potential distribution shown, would be

driven toward the sphere for the region from the sphere out to the place where the potential curve has a maximum. A charged particle would have no force exerted on it at the position of maximum potential (where the gradient or slope is zero) and then would be driven away from the sphere from position of maximum potential out to the boundary at ρ = 17.75 inches.

In Case I of Figure (17) the gradient is such that a charged particle of the same electrical sign as the cloud would move from the center outward.

If a neutral metal sphere were placed inside of the cloud and were isolated from any connection with a source of charge, we would find that it would assume the potential of the hole in the cloud made by the metal sphere, if the sphere were not present. This results from the definition of potential as given by Atwood (1).

> The absolute electric potential at any point in an electric field is the external work done upon a unit positive charge in moving it from a surface or region of zero electric potential to the point in the field.[1]

Thus it can be seen that it matters not whether a vacuum, other dielectric, or a conductor exist in the hole in the cloud, the potential or work required to bring a unit charge up to the point is the same. We will also find that at the cloud-sphere boundary the potential gradient is zero and thus no force is driving charged particles toward the metal sphere.

For the case of the sphere or other surface having a potential less than the potential of the neighboring cloud, the

---

[1]Atwood. Electric and Magnetic Fields. P. 37.

particles of the cloud will be driven toward the surface by action of the potential gradient (steepness of the potential curve) on the charged dust particle. Likewise if a surface (conducting or otherwise) possesses a potential greater than that of the surrounding cloud, we find the particle of charged dust driven away from that surface with no tendency to deposit. A consideration of the shape of the potential distribution shows that for Case I of the previous chapter the only tendency of the cloud is to disperse outward (considering electrical fields only).

For Case II where the potential on the sphere is above ground potential but much less than that of the maximum of the cloud, we see dust being driven onto the sphere within a spherical region having a radius of some 3.2 inches from center of metal sphere. At 3.2 inches radius from the sphere the particles experience no force at the instant the potential distribution is as shown. From 3.2 inches outward all of the charged dust is driven toward the outer boundary.

An instant after this distribution existed (for a free cloud), the potential distribution would have changed. The potential will seek to become the lowest possible constant value in the shortest time.

Even though plants may possess some small electrical surface charge, electrical dust deposition can be brought about as long as a potential gradient can be set up at the plant surfaces of sufficient magnitude to drive charged particles onto the plants.

There has been some discussion as to the effect of charged dust depositing onto the waxy surfaces of plants which have been shown to have a very high electrical resistance (amounting to several megohns per sq. cm.). This should be considered in the light of the magnitude of current being discharged by this type of deposition. The actual current carried in a depositing coat of dust is of the order of a fraction of a micro-ampere. If the surface resistance per square centimeter were some ten million ohms and one microamp was being deposited, the surface potential would be $E = IR = 10^{-6} \times 10^{7} = 10$ volts.

A glance at Case II of Figure (14) will show that the percentage reduction in potential gradient (field intensity) is roughly equal to the percent the surface potential is of the maximum potential of the cloud.

All of the previous discussions have concerned the potential distribution and forces acting in a uniformly charged static cloud, in other words, an imaginary cloud that could be formed and held for but a small fraction of a second, if at all. A study of the static cloud was necessary in order to understand the actual clouds that result in blowing dust into the vicinity of a growing plant.

The field forces of a charged cloud tend to reduce the density of a charged cloud in those regions where high potentials exist in the fastest manner possible. Thus the cloud attempts to assume the lowest possible constant potential and

does this as quickly as possible, consistent with the forces set up. A reasonably fair analogy would be the piling up of a very viscous fluid. When the pile has been released, the fluid moves into those places less deep than the peak of the pile, filling those places of little depth and closest to the peak more quickly than remote places with the fluid already at a moderate level.

In Case III of Figure (17) the forces are strongest nearest the metal sphere and become zero at a place of maximum potential and again moderately strong toward the outside of the cloud. If the electrical conductor to the grounded sphere and metal cage were disconnected at the instant the potential distribution as shown existed, the cloud would behave as follows: Because the forces are greatest at the sphere-cloud boundary, dust would be precipitated on the sphere.* Since there is no electrical connection to discharge the deposit, a surface charge results on the surface of the metal sphere giving rise to an increase in potential on the sphere surface. Meanwhile more charged dust has been moving into the region lately vacated by the deposited dust and doing so at the expense of the region near the maximum potential of the static distribution. Also, charge has been moving out less fast to the cage and it begins to raise in

*This is not the case of an isolated sphere that was neutral to begin with. This sphere had a negative charge on it when the electrical connections were broken.

potential due to dust deposition. In time we would have a charge density such that a constant potential would exist throughout the cloud and on the boundary surfaces. The charge would then all be on the boundary surfaces. The increase of charge density near the boundaries tends to raise the potentials near the boundaries and thus if the surfaces discharge the charge brought with the depositing particles, the gradients will be considerably increased above the uniform charge density condition. This condition has been noted by the writer as evidenced by field intensities of such magnitude at the surface of a disk parallel to the flow of charged dust stream, that a slight crackling and a faint blue discharge were observed when the dust cloud was blown past the grounded disk.

Deposit Test

We now have a theory of dust deposition which states that if the potential on the object to be coated is less than that of the surrounding cloud, a coat of dust will be deposited. Also, if an initially uncharged sphere is isolated and surrounded with a charged cloud of dust, no electrical deposition will take place. The deposit test was made to test this theory.

A number of aluminum foil spheres were constructed as shown in Figure (19). These metal spherical shells were

approximately .95 inch diameter with a small flange of about one-sixteenth of an inch width. The flange was elongated as shown, on opposite ends to provide space for a small hole. A small wire hook was passed through the top hole and a weight on the end of a nylon fishline leader was hooked into the bottom end of the metal sphere. For the isolated sphere the top hook was supported on the end of a length of nylon fishline leader which acted as an insulating support. For the grounded sphere the support was provided by a fine copper wire within a spaghetti tube, which also acted as the electrical contact with the ground. The weight that was suspended from the bottom of the metal shell was used in order to prevent the very light shell from bobbing around due to the turbulence within the chamber. This weight also kept the metal spherical shell in the center of the spherical cage. The same equipment was used for this test as for the previous tests for measuring potential.

The procedure used for this test was as follows: The exhaust fan outlet was in full closed position. The axial flow fan was positioned as shown in Figure (12). The variac supplying input to the high voltage power supply was set at 80. The high voltage power supply was delivering positive current. The charge density was kept as uniform as possible by using the gold leaf electroscope calibrated for 400 volts. The probe to the electroscope was positioned one inch from the top of the wire cage. The blower was operated at 2,500

r.p.m. and the dust used was micronized attaclay. A 24 gram sample was fed into the blower by hand. The rate of feeding was governed by the potential indicated by the leaf of the electroscope. An attempt was made to maintain the voltage at 400 volts. This was possible about ninty percent of the time. When not on 400 volts the leaf was either above or below usually not more than 50 volts either way.

The blower, charging nozzle and the measuring chamber were all thoroughly cleaned out between runs.

There were two treatments and four replications of each. The eight replications were randomized as to order of performance of runs. The time required to run the entire charge of 24 grams of dust through the chamber with the potential at 400 volts was also noted to catch any large changes in charging rate. The lower the charge level on the dust particles, the faster the rate of feeding to maintain the 400 volt potential. This would result in a shorter time of run. It is not now apparent whether or not this would measurably effect the rate of the deposit.

Evaluation of deposit was accomplished by weighing on an analytical balance CENCO IU 1748 direct reading to .0001 g.

In performance of a run, three of the metal shells were carefully weighed and placed on hooks in a cigar box as shown in Figure (20). The cover was closed before the metal shells were transported to the building where the test work was carried out. Then a metal sphere was carefully placed on the

appropriate suspension within the spherical cage. The suspension that was not used for a given run was placed out of the way during the run. The weight was then suspended from the bottom of the metal shell. Access to the inside of the wire sphere was obtained by a hinged opening in the wire. This was secured in its proper place before a run was made.

After the run was completed the metal shell was carefully removed with tweezers and placed again on a hook in the cigar box. The positions of the metal shells were identified in the box and only one shell was removed at a time.

The following table gives the results of each run and the order in which they were run. Treatment A is for the isolated case and treatment B is for the grounded case.

TABLE XV

DATA SHEET FOR DEPOSIT TEST

Run No.	Treat. & Rep.	Total time for run	Total wt. gms.	Tare gms.	Dust weight gms.
1	A 1	19 min.	0.3987	0.3984	0.0003
2	A 2	18 min.	0.3944	0.3942	0.0002
3	B 1	16 min.	0.3941	0.3929	0.0012
4	A 3	18 min.	0.3906	0.3905	0.0001
5	B 2	17 min.	0.3988	0.3974	0.0014
6	A 4	16 min.	0.3966 +	0.3963	0.0003 +
7	B 3	14 min.	0.3988	0.3977	0.0011
8	B 4	16 min.	0.3987	0.3973	0.0014

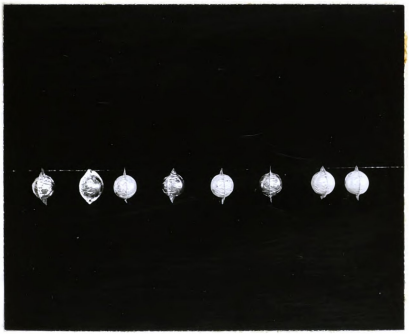

Fig. 19. View of metal shells in order of run of deposit test.

Fig. 20. Carrying box for deposit test.

For treatment A the sample mean is

$$\bar{x} = \frac{.0003 + .0002 + .0001 + .00032}{n} = .00023 \text{ gms.}$$

Standard error $s = \sqrt{\frac{\Sigma x^2}{n-1}} = .0001$ gms.

$= .00005$ gms.

Error of the mean $S_{\bar{x}} = \frac{S}{\sqrt{n}}$

$t_{.05}$ for three degrees of freedom = 3.182

Fiducial limits of the mean m

$l_1 = \bar{x} + t_{.05} \times S_{\bar{x}} = .00023 + 3.182 \times .00005 = .00039$ gms.

$l_2 = .00023 - 3.182 \times .00005 = .00007$ gms.

For treatment B

$$\bar{x} = \frac{.0012 + .0014 + .0011 + .0014}{n} = .00127 \text{ gms}$$

$$S = \sqrt{\frac{\Sigma x^2}{n-1}} = .00015 \text{ gms.}$$

$$S_{\bar{x}} = \frac{S}{\sqrt{n}} = \frac{.00015}{\sqrt{4}} = .000075 \text{ gms.}$$

$l_1 = .00156$ gms.

$l_2 = .00098$ gms.

Discussion of Results

As can be noted from the preceding page, the sample mean for treatment B (the grounded sphere) was 0.00127 gms. as compared to the sample mean of 0.00023 gms. for treatment A. On the basis of the theory the mean for treatment A should have been zero but in all cases there was a small number of large clots of dust that dropped down from the wire of cage above during the run and in handling after the run. These clots appeared on all shells to some degree. Although the cage was cleaned before each run, it collected dust in considerable amounts because of the high field intensities associated with the fine wires.

The population mean at the 95 percent confidence level should lie between $m = 0.00127 \pm .00029$ gms. for treatment B and $m = 0.00023 \pm .00016$ gms. for treatment A.

The minimum fiducial limit of treatment B is more than twice that of the maximum fiducial limit of treatment A at the 95 percent confidence level. No actual dust deposit other than the clots due to gravity were detected on the shells of treatment A. The very high metallic lustre on the shells of treatment A attests to the absence of more than a few small particles collected by electrical deposition. The treatment B shells had a very uniform coating of very fine dust which greatly dulled the natural metallic lustre of the uncoated shells.

It is the author's belief that the deposition theory has been verified to the extent that deposition occurs as long as the collecting surface is kept at a lower potential than the surrounding cloud and that an isolated conductor will assume the potential of its surroundings and, therefore, collect no dust due to electrical forces.

The Electric Field and Potential Distribution of a Finite Disk and a Finite Cloud

The study of spherical clouds enveloping a metal sphere has served to verify the methods of electric field analysis but in themselves have little to merit as regards agricultural crop dusting.

The electric fields of interest are those that are found next to the leaves and stems of agricultural crop plants when a cloud of charged dust is blown into the inner plant regions.

A complete analysis of the field surrounding a plant leaf would be difficult indeed and probably would not be worth what it would cost in time and effort. However, an analysis of the forces that occur along a perpendicular axis of a small disk when a cylindrical cloud of dust is next to it would be of considerable help. This would give the minimum force that would be available to a leaf, as all other areas of the leaf would usually have as large or larger forces active.

By use of two formulas developed in potential theory for the force along the axis of a cylindrical charged cloud of uniform density, and the use of the principles of imaging and superposition, one may construct the field intensity distribution along a perpendicular axis of a conducting disk.

The fields to be constructed are those of a four inch diameter conducting disk with a cylindrical cloud four inches in diameter and four inches high placed in contact with it, Figure (21), and a four inch high cylindrical cloud sandwiched between two four inch diameter conducting disks at zero potential, Figure (22).

The following pages show the steps used in constructing these fields.

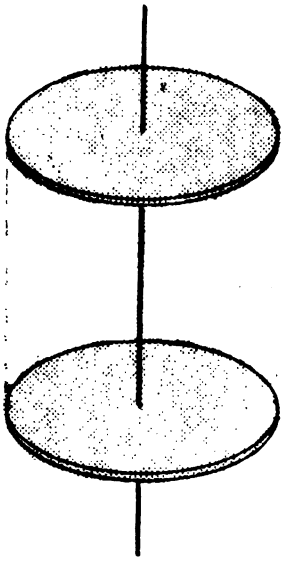

Fig. 22. Cloud sandwiched between 2 disks at zero potential.

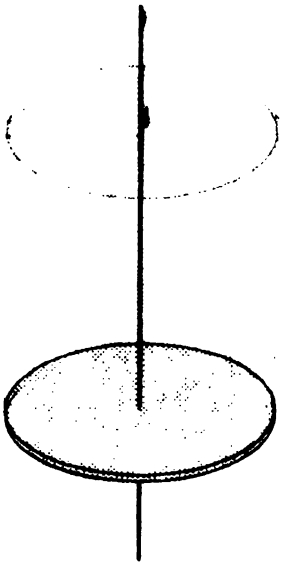

Fig. 21. Cloud next to a single disk at zero potential.

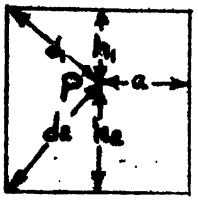

Fig. 23. Diagram showing constants for formula. $F = 2\pi\rho(h_2 - h_1 + d_1 - d_2)$, Force on particle with unit + charge for Figures 25, 26, 27, 28 and 29.
$d_1 = \sqrt{h_1^2 + a^2}$, $d_2 = \sqrt{h_2^2 + a^2}$

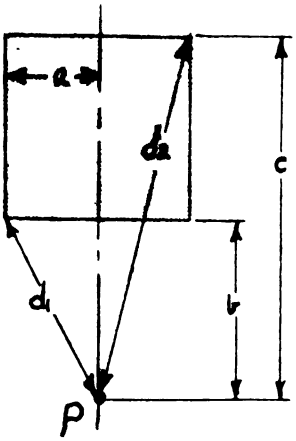

Fig. 24. Diagram showing constants for formula.
$F = 2\pi\rho(h + d_1 - d_2)$, Force on a particle with unit + charge for Figures 30, 31, 32 and 33.
$h = (c - b)$, $d_1 = \sqrt{a^2 + b^2}$,
$d_2 = \sqrt{a^2 + c^2}$

Fig. 25.

$F = 2\pi\rho\,(h_2 - d_2 + a)$

$F = 2\pi\rho\,[4 - \sqrt{20} + 2]$

$F = 2\pi\rho\,[6 - 4.48]$

$F = 9.55\,\rho$

$h_1 = 0$

$h_2 = 4$

$d_1 = a = 2$

$d_2 = \sqrt{2^2 + 4^2}$

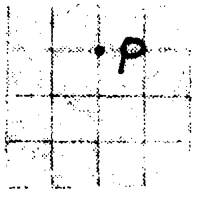

Fig. 26.

$F = 2\pi\rho\,(h_2 - h_1 + d_1 - d_2)$

$F = 2\pi\rho\,(3 - 1 + 2.25 - 3.61)$

$F = 2\pi\rho\,(.64)$

$F = 4.02\,\rho$

$h_1 = 1$

$h_2 = 3$

$d_1 = \sqrt{2^2 + 1^2}$

$d = \sqrt{2^2 + 3^2}$

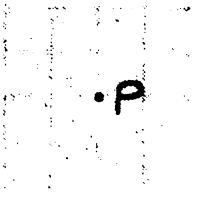

Fig. 27.

$F = 2\pi\rho\,(h_2 - h_1 + d_1 - d_2)$

$F = 2\pi\rho\,(2 - 2 + \sqrt{2^2 + 2^2} - \sqrt{2^2 + 2^2})$

$F = 0$

$h_1 = 2$

$h_2 = 2$

$d_1 = \sqrt{2^2 + 2^2}$

$d_2 = \sqrt{2^2 + 2^2}$

$$F = 2\pi\rho[h_2 - h_1 + d_1 - d_2]$$

$$F = 2\pi\rho[1 - 3 + \sqrt{13} - \sqrt{5}]$$

$$F = 2\pi\rho[1 - 3 + 3.61 - 2.25]$$

$$F = -4.02\rho$$

$h_1 = 3$

$h_2 = 1$

$d_1 = \sqrt{2^2 + 3^2}$

$d_2 = \sqrt{2^2 + 1^2}$

• P

Fig. 28.

From symmetry with (25) the force is

$$F = -9.55\rho$$

• P

Fig. 29.

Fig. 30.

$h = 4 = c - b$

$$F = -2\pi\rho[h + d_1 - d_2]$$

$$F = -2\pi\rho[4 + \sqrt{5} - \sqrt{29}]$$

$$F = -2\pi\rho[4 + 2.25 - 5.39]$$

$$F = -2\pi\rho[6.25 - 5.39]$$

$$F = -2\pi\rho[.86]$$

$$F = -5.4\rho$$

$d_1 = \sqrt{1^2 + 2^2} = 5$

$d_2 = \sqrt{5^2 + 2^2} = 29$

• P

Fig. 31.

$F = -2\pi\mu\rho\,[h + d_1 - d_2]$ $\qquad h = 4$

$F = -2\pi\mu\rho\,[4 + \sqrt{8} - \sqrt{40}]$ $\qquad d_1 = \sqrt{2^2 + 2^2} = \sqrt{8}$

$F = -2\pi\mu\rho\,[4 + 2.83 - 6.34]$ $\qquad d_2 = \sqrt{6^2 + 2^2} = \sqrt{40}$

$F = -2\pi\mu\rho\,[6.83 - 6.34] = -3.08\,\mu\rho$

•P

Fig. 32.

$F = -2\pi\mu\rho\,[h + d_1 - d_2]$ $\qquad h = 4$

$F = -2\pi\mu\rho\,[4 + \sqrt{13} - \sqrt{53}]$ $\qquad d_1 = \sqrt{2^2 + 3^2} = \sqrt{13}$

$F = -2\pi\mu\rho\,(4 + 3.61 - 7.29]$ $\qquad d_2 = \sqrt{2^2 + 7^2} = \sqrt{53}$

$F = -2\pi\mu\rho\,[7.61 - 7.29] = -2.01\mu\rho$

•P

Fig. 33.

$F = -2\pi\mu\rho\,[h + d_1 - d_2]$ $\qquad h = 4$

$F = -2\pi\mu\rho\,[4 + \sqrt{20} - \sqrt{68}]$ $\qquad d_1 = \sqrt{2^2 + 4^2} = \sqrt{20}$

$F = -2\pi\mu\rho\,[4 + 4.48 - 8.25]$ $\qquad d_2 = \sqrt{2^2 + 8^2} = \sqrt{68}$

$F = -2\pi\mu\rho\,[8.48 - 8.25]$

$F = -2\pi\mu\rho\,[.23] = -1.44\,\mu\rho$

•P

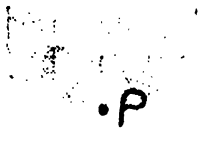

Fig. 34.

$F = 2\pi\omega(2 + \sqrt{4} - \sqrt{8})$

$F = 2\pi\omega(4 - 2.82)$

$F = 7.4\,\omega$

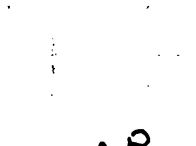

Fig. 35.

$F = 2\pi\omega(2 + \sqrt{5} - \sqrt{13})$

$F = 2\pi\omega(4.24 - 3.60)$

$F = 4.02\,\omega$

Fig. 36.

$F = 2\pi\omega(2 + \sqrt{8} - \sqrt{20})$

$F = 2\pi\omega(4.82 - 4.48)$

$F = 2.14\,\omega$

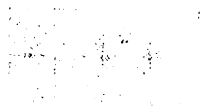

Fig. 37.

$F = 2\pi\rho(2 + \sqrt{13} - \sqrt{29})$

$F = 2\pi\rho(5.6 - 5.4)$

$F = 1.26\rho$

• P

Fig. 38.

$F = 2\pi\rho(h + d_1 - d_2)$

$F = 2\pi\rho(2 + \sqrt{20} - \sqrt{40})$

$F = 2\pi\rho(6.48 - 6.30)$

$F = 1.13\rho$

• P

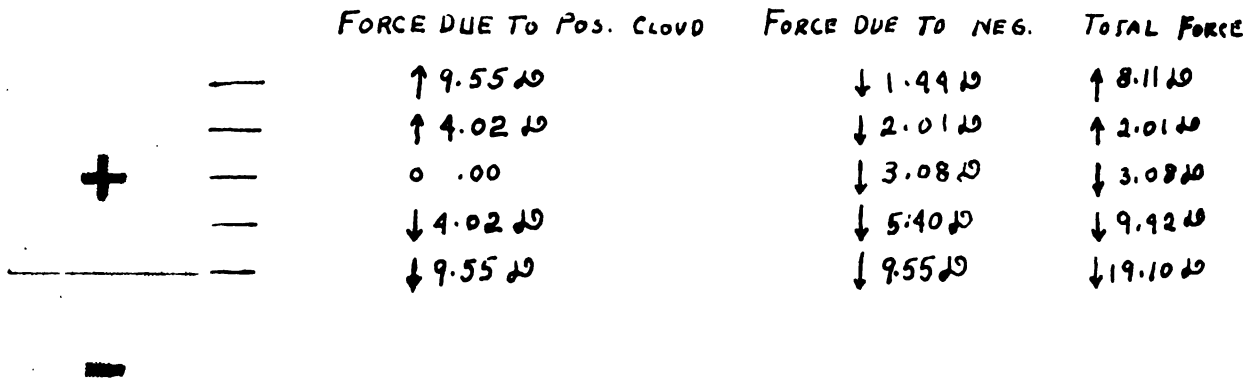

Fig. 39. Development of the force experienced by a unit charge placed along the perpendicular axis in a positive cloud near a conducting disk at zero potential.

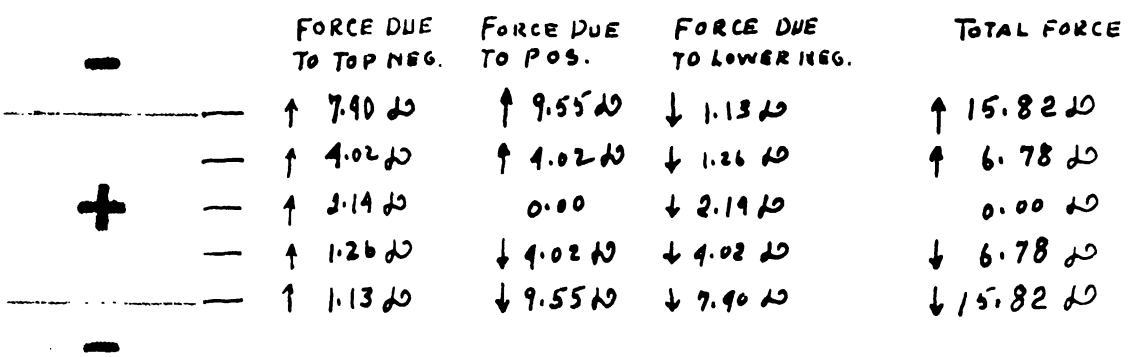

Fig. 40. Development of the force experienced by a unit charge placed along the perpendicular axis in a positive cloud between two conducting disks at zero potential.

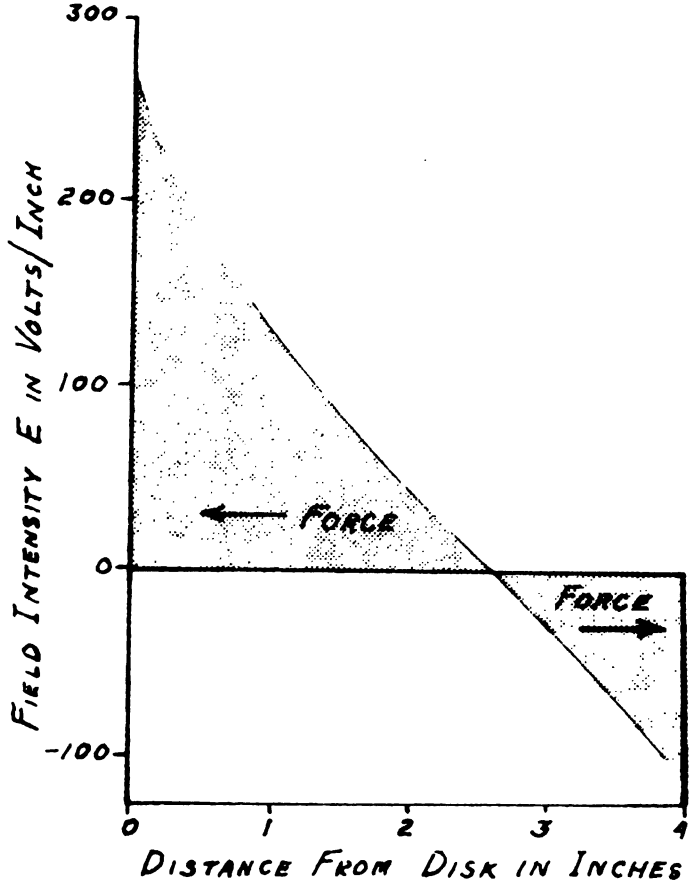

Fig. 41. Field intensity along axis of cloud next to the single conducting disk at zero potential of Fig. 21. The force direction is that of one of population of a uni-signed cloud. Charge density ρ = 13.75.

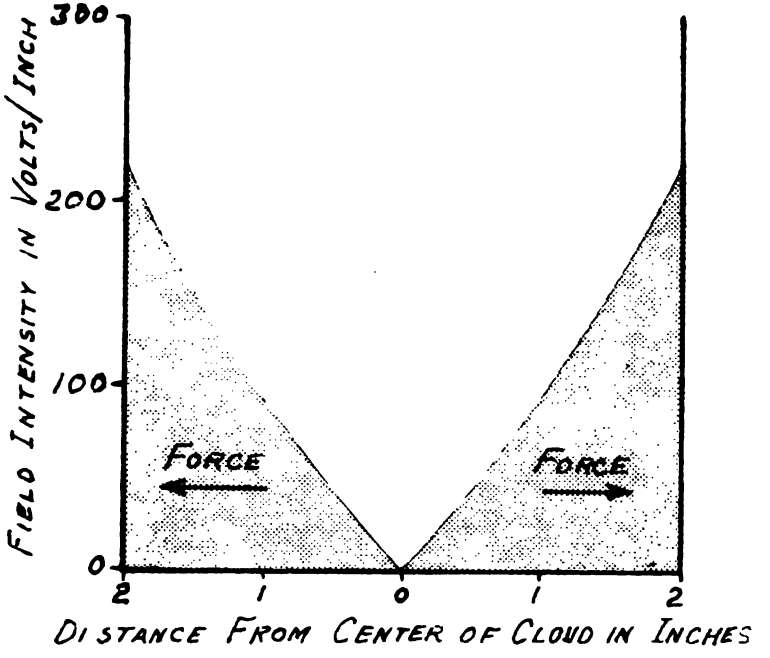

Fig. 42. Field intensity along axis of the cloud sandwiched between the two conducting disks at zero potential of Fig. 22. Force direction is that of one of the population of a uni-signed cloud. Charge density ρ = 13.75.

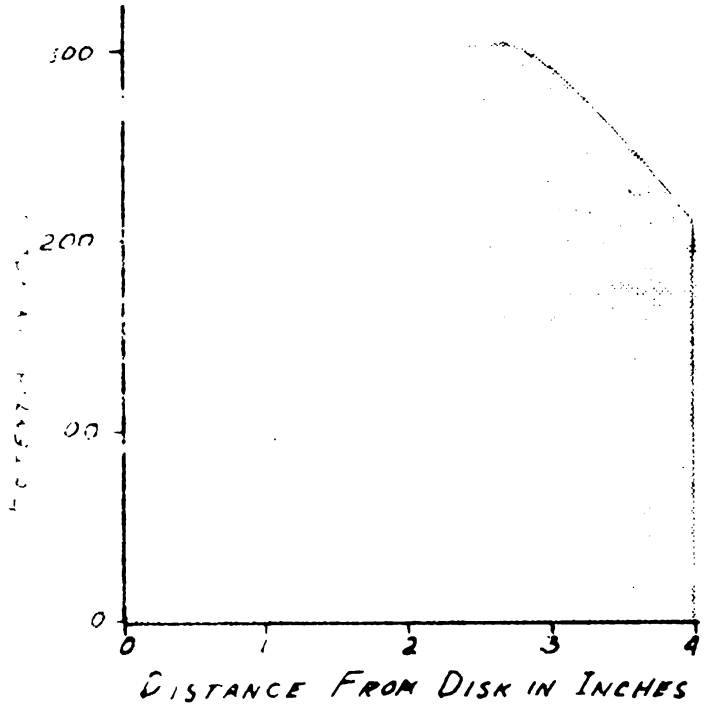

Fig. 43. Potential distribution along axis of cloud shown in Fig. 21.

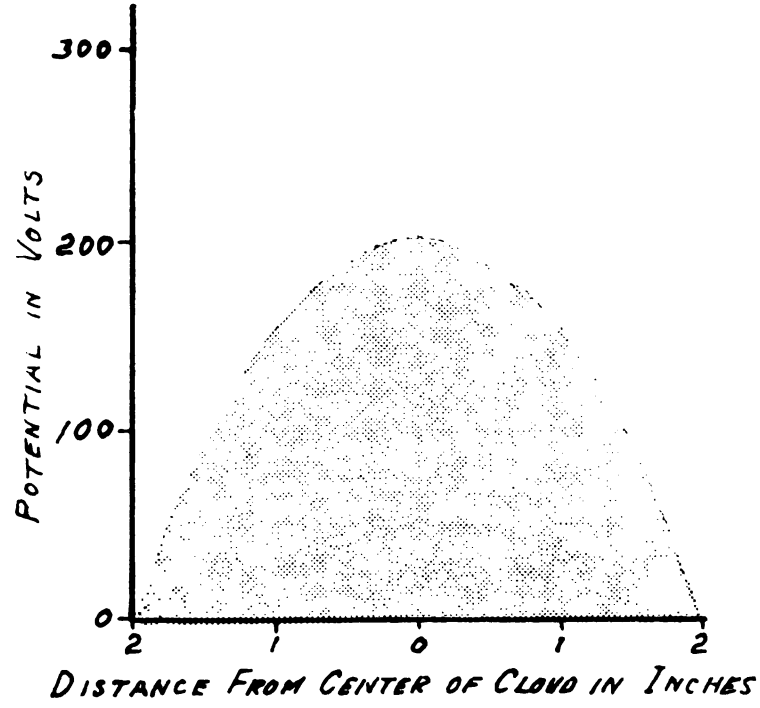

Fig. 44. Potential distribution along axis of cloud shown in Fig. 22.

The force F as calculated is the force on a unit positive charge and thus is equal to the field intensity. The direction of the force is the direction a positive charge would be urged if placed in the position under consideration. Thus at the top or bottom of a positive cloud a positive charge would be urged away from the cloud. At the center of a positive cloud no force would act upon the positive particle. A positive particle would be urged toward the center of a negative charge distribution.

A view of Figure (41) shows that the maximum force occurs near the surface of the disk, and acting to move a positive particle to the surface gradually diminishing until at a distance approximately two-thirds of height of cylinder from disk. There the force is zero and for the rest of the distance to the outside boundary of the cloud we find the field urging a positive particle outward and away from the surface. This considers a zero boundary at infinity. This condition is approximated by a cloud next to the outside leaves of a plant in field work.

The potential distribution, Figure (43), may be constructed by the addition of the average intensities for each successive point. The potential and intensity distributions have the same general shape as did those of a spherical cloud when the central sphere is large and the cloud envelope thin. A study of either this or the spherical case will show that the potential distribution and field intensity magnitude are very dependent upon the thickness of the dust cloud blanket for a

given charge density. Both an increasing of charge density and an increase in the thickness of the blanket will increase the potential maximum and magnitude field intensity at the disk surface. Of course this will prove to be important in considerations of very close spaced leaves. A second important field is that of a cloud sandwiched between two parallel leaves, as this condition is the rule rather than the exception in the inner regions of the plant. Figure (42) shows the intensity distribution and Figure (44) shows the potential distribution for this case. The maximum intensity at the surface has been reduced by about twenty percent and now the position of zero force is midway between the disks, and the potential distribution is symmetrical as one would expect.

The field forces available in this boundary configuration are very feeble compared to the forces available for the case of the sphere surrounded by a thick cloud. No doubt this accounts for the inability of the workers to transfer to the field the almost unbelievably good results obtained when a charged cloud is blown around an apple. The thickness of the cloud envelope is in a large measure responsible for this. The general form of the field will remain the same regardless of the thickness of the cloud.

A comparison of the forces available for the above cases as well as for the metal sphere and spherical cloud will be made with inertial and gravity forces in the next section.

INERTIAL FORCES IN A MOVING DUST CLOUD

Review of Literature

A review of literature has not disclosed a solution to this problem except in some special cases that do not apply directly to a clear understanding of particle deposition in pesticide application.

According to Brooks (5), a development by Langmuir has shown that the inertial or dynamical catch of aerosol droplets is directly related to the size of the particle and velocity of the airstream carrying and inversely related to the diameter of the collecting cylinder. His work was done in relation to the collection of water droplets on airplane wings passing through clouds.

A method of plotting the trajectories of water droplets as air passes around a wing profile has been developed by Bergrun (3) using numerical integration. This method is valid when the streamlines are known. This latter method deals with free airstream velocities of the order of 300 miles per hour or greater in the region where incompressible fluid calculations are definitely invalid and the streamline and Reynolds numbers are such that Stoke's law is not even a close approximation. The method outlined in the above article

will yield a more accurate solution than the one about to be executed, but requires a familiarity with the mathematics of numerical methods and a considerable amount of time.

Discussion of Force

According to Newton's second law, a body in motion continues to move in a given direction without diminishing velocity until acted upon by an external force. The resistance to change of motion in a straight line is known as inertia and the amount of force required to overcome this inertia is the time derivative of the change in linear momentum of a given body. One of the most important of forces operating in the deposition of particles out of the air stream conveying them is the inertial force. An inertial force is produced on a particle when an air stream is deflected by a surface and the linear momentum of the particle carries it toward the surface.

The particles dealt with in dusting work are usually passed through a 325 mesh screen (44 microns opening) and usually vary in size from 1/2 micron to 44 microns in their largest transverse crossection diameter. The active ingredients in dusts are generally in the range of 1/2 to 20 microns because of the methods of manufacture and or subsequent treatment. Since a given amount of poison can be spread over much greater area and many materials are greatly increased

in activity, it is generally believed and has been demonstrated in laboratories that less material is required to control a pest when the material is relatively fine than when coarse. The active particles of interest are for the most part those in the 10 to 20 micron range. That is to say, this range is a compromise between the advantages of larger surface coverage of small particles and the inertia and resistance force advantages in deposition of larger particles.

Statement of the Problem

The problem is to determine the net force that is active in driving a particle toward a surface when the air stream conveying the particle is deflected by the surface.

Assumptions Necessary

In order for this problem to be solved with any reasonable amount of labor certain assumptions must be made to simplify the problem.

(a) The system is two dimensional.

(b) The air is carried around the obstructing surface in streamline flow.

(c) The streamlines are parallel within the regions of interest (that is region of particle path).

(d) The particles are spheres.

(e) The streamline and particle path line are coincident just before the deflection occurs.

(f) That Stoke's law is valid over the range of action considered.

All of the above assumptions lead to errors, but these can be kept small providing certain requirements are met as regards the size of particles, velocity of particle movement with respect to air, velocity of air movement past the deflecting surface and smoothness of the surface.

Two Dimensional Problem.

The actual streamlines formed around a finite surface are three dimensional and according to Prandtl (10) are cubic hyberbolas of the form $x\,y^2 =$ constant which are rotationally symmetrical about the z-axis as shown in Figure (45). The projection of the streamlines on the x-y plane are of the form shown in Figure (45). This type of flow is that that would be expected if a large diameter jet of non-compressible fluid impinged upon an infinite plane. The mathematics of this type of flow is somewhat complicated and will not be carried out at this time. In two dimensional flow on the other hand, the streamlines all lie in the x-y plane and the object around which the fluid is flowing is long as compared to its cross-section. When the fluid flows in two dimensions the streamlines will be as indicated in Figure (46) for impingment of

fluid against a flat plate. A comparison of the flow for a two dimension plate and a three dimension plate shows a difference in streamlines of quite some importance in particle deposition. However, limited time has dictated that the two dimensional flow be done first and later three dimensional work will be done since there are mathematical complications in the three dimensional form that must be eliminated before successful computation is possible. A great deal can be learned of the order of magnitude of the forces involved from the two dimensional case and the characteristics caused by changing values of mass and velocity of particle and air-stream will be the same for two dimensional and three dimensional flow. As a further simplification to get the method an approximation to the path, a circular path is substituted for the hyperbolic path of two dimension flow. This is justifiable on the basis that it will afford a great deal of information for a fairly reasonable time expenditure.

Streamline Flow.

Streamline flow or potential flow means that the fluid does not go into vortices and break away from the obstacle past which it is flowing, Figure (47). Streamlines give a plot of the velocity direction at each point in the field. According to Prandtl (11) gases may be treated as non-compressible as far as streamline form are concerned as long as the

velocity of the gas is kept within reasonable limits. For air at atmospheric pressure and at a temperature of 15° C an error in the form of the streamline reaches 1.0 percent when the velocity reaches 160 ft./sec. Since the density decreases as velocity increases in the following fashion from Prandtl (11).

$$\rho = \rho_o \left(1 - 1/2 \frac{W^2}{C_1^2} + \ldots.\right)$$

where W = velocity of air and C_1 = velocity of sound in the gas, the change in density is introduced by the second term in the above formula. It is a function of the velocity squared and the error at 1 percent is found by setting the second term to .01. The velocity of sound in air at the above conditions is equal to 1120 ft./sec. so that by setting

$$.01 = \frac{W^2}{2C_1^2}$$

$$W = \sqrt{.02C_1^2} = \frac{C_1}{10}\sqrt{2} = 160 \text{ ft./sec.}$$

Studies of dusting and spray work will lie within the air velocities where the streamlines will not depart by more than 2 percent since this will give a maximum velocity of 226 ft./sec. which is approximately 152 miles/hr.

Except for those leaves directly in front of a duster nozzle where the velocity may be as high as 125 miles/hr., the velocities will be considerably less and will not exceed 20 miles/hr., except in a very narrow band, according to

measurements by Barnes (2).

In a great majority of the plant regions the velocities directed perpendicular to the surfaces will not exceed 10 miles per hour and may be much less at which condition the compressibility of air will not change the form of the streamlines more than a fraction of 1 percent. Except for the region near the boundary surface, the flow will be streamline and of a form considering the gas as non-compressible.

Behind the surfaces there is a dead region formed, Prandtl (11), where the pressure is that of the undisturbed fluid as in Figure (48).

Parallel Streamlines.

Parallel streamlines are assumed in order for the calculation to be carried out without a step by step numerical integration. The streamlines that are crossed will be considered parallel. If the distance travelled by the particle away from a given streamline is relatively small, this will not introduce large errors; however, for very large distances across streamlines this can be large and must always be considered when analyzing the results.

Spherical Particles.

Spherical particles have been very thoroughly investigated as regards their movement through fluids because of the relatively simple mathematics involved. However, other shaped

particles have been experimentally studied and can be related to an equivalent spherical particle by means of suitable coefficients.

> In general, the relationship for spheres holds fairly well (within ± 20%) for irregular particles for values of N of less than 50 where the particle shapes are not extreme and where the diameter as measured by screens, elutriation, microscope, or otherwise is taken as the diameter of an equivalent sphere.[1]

The Streamline and Particle Paths are Coincident.

The streamline and particle paths are coincident and the velocity of the particle is equal to the velocity of the stream at time just before disturbance of free flow begins. This is almost strictly true for motion where the air and particles are not being accelerated. Here gravity forces have been considered small or acting perpendicular to the plane of the streamlines.

Stokes Law as an Approximation for the Resistance to Motion Through Air.

According to Lapple (8) Stokes law is a good approximation in the range where R_p is less than 2, and the velocity does not exceed a certain value for a given particle diameter. The values of R_p, the value of the drag coefficient C, and the velocity of relative movement of particle and air are all

---

[1] Lapple. Fluid and Particle Mechanics. P. 288.

such that Stokes law $F_r = 3\pi u D_p \mu$ does not vary over the whole range of values of u encountered in the example from the true $F_r = \frac{\pi D_p^2 \rho C u}{8}$ by more than a few percent.

Development of particle path derivation from the equation of the path circular streamlines of a spherical particle can be evaluated approximately provided the equation of the particle path is known in terms of the time t.

According to Lapple and Shepherd (9), for streamline flow the motion is Newtonian and the motion in the x direction may be superposed on the motion in the y direction and the resultant gives the actual particle path. The equation developed in Appendix III gives the path of a spherical particle of density 2 and diameter 20 microns. This particle approaches a surface perpendicular to the flow as shown in Figure (46), and the true hyperbolic streamline is approximated by a quarter circle, Figure (49). The set-up is shown in Figure (49), and the path and manner in which the particle departs from it is shown in Figure (50).

The streamline path flowing around a flat plate would have a form as in Figure (47) if the fluid were perfect, that is had no viscosity. In a real fluid with viscosity there is a separation of the boundary layer behind the plate and there is a turbulence in that area with a slightly lower pressure than that of the free stream. In front of the plate, however, the streamlines approach those of the perfect fluid when the plate is smooth. This type of flow is pictured in Figure (48).

We are interested in what happens to a particle of dust as it is carried by the streamline as pictured in Figure (48). This part of the streamline is represented by $xy = 6$, Figure (46), a streamline that at 1 cm. from x-axis is 6 cm. from y axis and further is almost perfectly represented by a circle of radius 5 cm. The density of our particle is taken to be 2, its diameter is 20 microns and it is a sphere. The velocity of the free stream is taken to be 450 cm./sec. (approximately 10 MPH).

The streamlines are taken to be parallel as in Figure (49). A better approximation would be concentric circular streamlines, but this would require step by step numerical integration.

The parametric equations for the particle paths are equal to the following:

$$x(t) = -6 + 1 + .964\,(5 \sin wt - \cos wt) - .036\, e^{-\frac{k}{m}t}$$

$$y(t) = 6 + .0225 - .964\,(5 \cos wt + \sin wt) - .1925\, e^{-\frac{k}{m}t}$$

Values of $x(t)$ and $y(t)$ are now plotted for values of t and yield the plot of Figure (51).

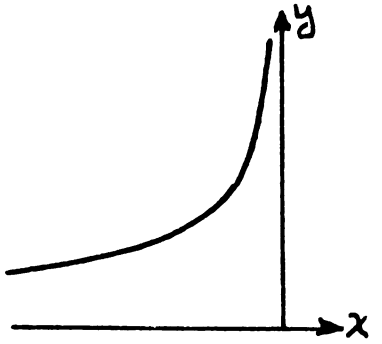

Fig. 45. Streamline of 3-dimensional flow $xy^2 = C$.

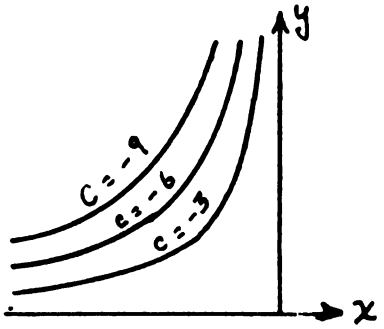

Fig. 46. Streamlines of 2-dimensional flow $xy = C$.

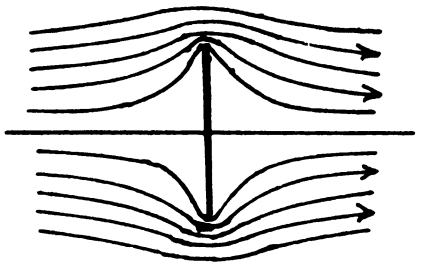

Fig. 47. Streamlines for 2-dimensional potential flow around a flat plate.

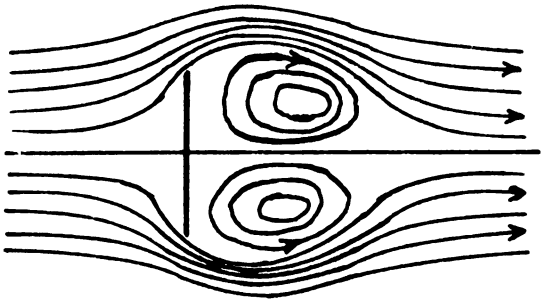

Fig. 48. Streamlines for 2-dimensional viscous flow around a flat plate.

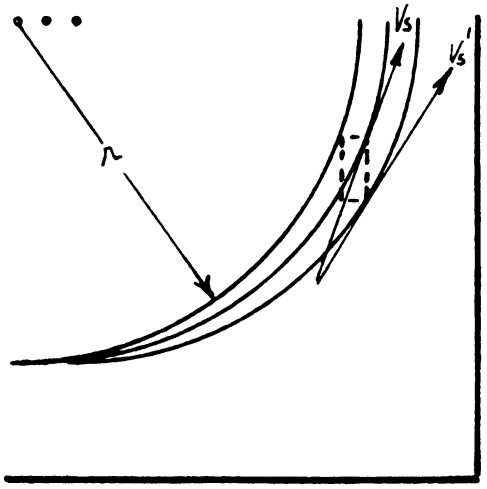

Fig. 49. Relation of V_s used in formula $\ddot{x} + \frac{k}{m}\dot{x} = \frac{k}{m} V_{sx}$ and actual V_s' that the particle would experience due to y-component of inertia.

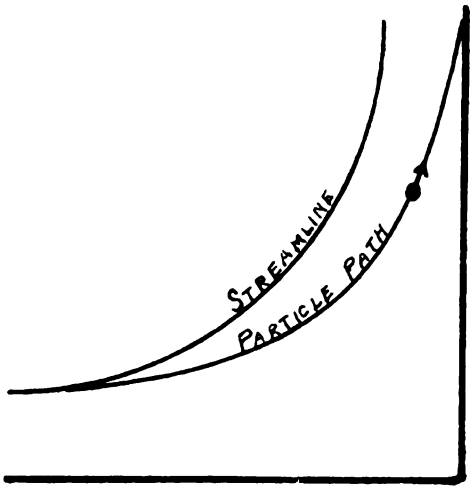

Fig. 50. Manner in which particle path deviates from circular streamline.

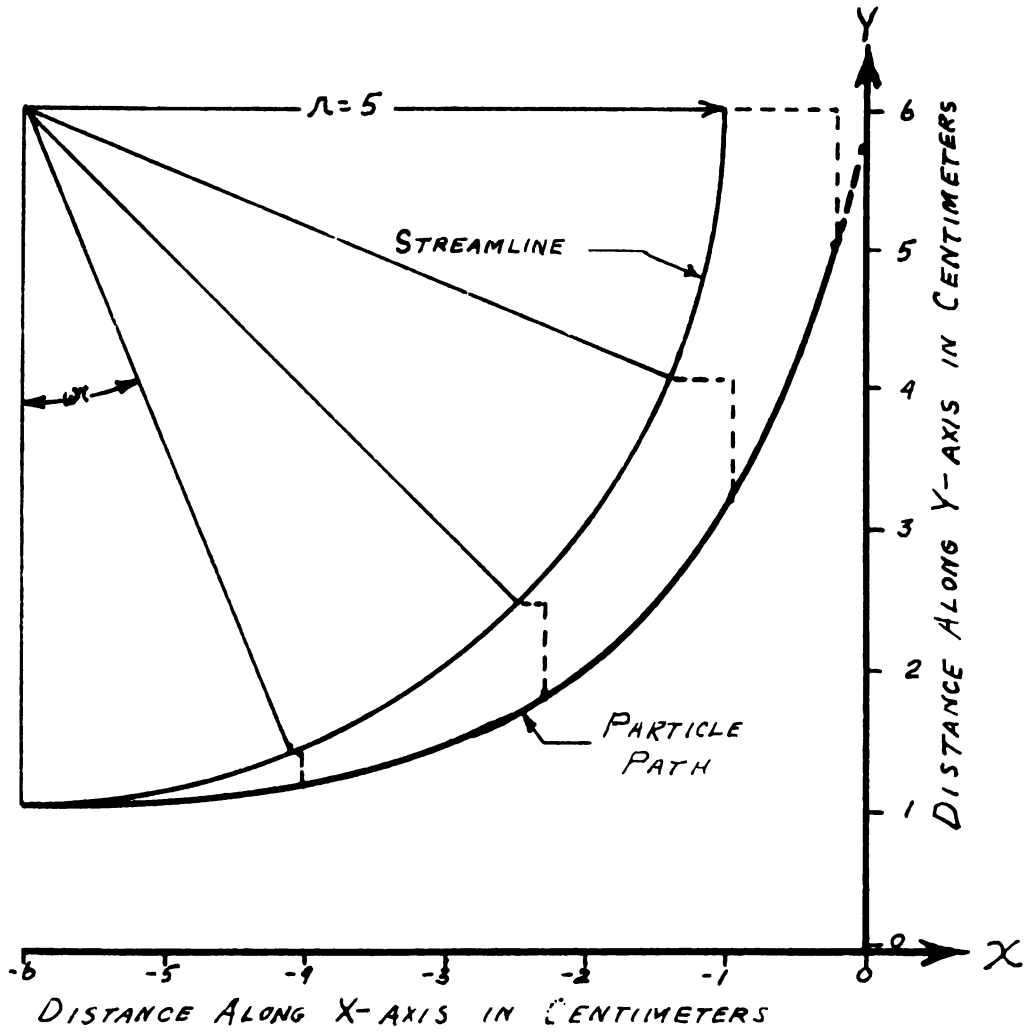

Fig. 51. 20 micron particle deviation from circular streamline of 5 cm. radius with streamline velocity vs equal to 450 cm/sec and the particle density equal to 2.

Discussion of Results

A study of Figure (49) will show that for the circular case calculated in Appendix III, the V_s of the streamline as used in the analysis has a smaller x-component than does the V_s' of the particular circular streamline on which the particle finds itself due to the y-component of the inertia. Thus the x-component of the deviation from the original circular path would be in the neighborhood of 25 percent larger than the deviation as given. However, a look at Figure (46) will show that as we approach the surface the streamlines themselves have a smaller x-component of velocity for a given value of y and thus there is a compensation for the increased x-component of velocity of streamline.

The calculation based on a circular streamline is thus more valid for the real case than for the circular streamlines. Another factor is that because of varying Reynolds numbers the particles are subjected to greater drags at times than is indicated by Stoke's laws. However, assuming the equations of motion are reasonably close, the drag forces do not vary from Stoke's law by more than a few percent at any time.

It is the opinion of the writer that the equations of motion are a good approximation to the true deviation of particle from the streamlines and that the order of magnitude deviation in the x-direction for a 20 micron spherical particle under the conditions previously described, is one centimeter.

The substance of the aforewritten is that the final position of the particle is very nearly correct, but the true path would deviate somewhat from that shown. This indicates that a particle of these specifications in the stream one centimeter from the perpendicular axis of a long plate twelve centimeters wide would just be caught by the surface. All particles of this size within one centimeter of the x-axis should be caught. All those more than one centimeter from the axis would pass by this surface without striking the surface.

This means that at 10 miles per hour velocity only about 17 percent of the particles of 20 microns diameter and density of 2 would strike the surface. The rest would go around the surface. A decrease in mass of the particle such as reducing the density would reduce the path deviation from the streamline in linear fashion. Half the mass would give half the deviation. An increase in velocity would increase the path deviation and the percentage of particles caught. Smaller particle sizes with their increased drag and decreased inertia will take a decreased deviation that will vary approximately as the square the ratio of the size. That is, a ten micron particle will deviate approximately one-quarter as much as the twenty micron particles. This means only about 4 percent of the particles in the projected area of the surface across the stream would strike the surface.

The foregoing discussion would be reasonably valid for those cases in which a collecting surface was moved through

an essentially undisturbed suspension of particles, such as for an airplane moving through a cloud or a plate moved through a room full of a suspended aerosol. Brooks (5) has transferred material from the field of aeronautics, as has the author in this paper, and has used it to calculate the deposition efficiency and explain the phenomena that takes place in ordinary dusting and plant pesticide work.

It is believed by this author after considerable reflection and a scrutiny of the laws governing the resistance forces acting, that the resistive forces to the passage of a particle through a fluid is very greatly modified (decreased) because of general turbulence within the fluid carrying the suspended particles. Turbulence within the fluid breaks down the shear forces in such a manner that the particle acts as though it were in a medium of lower viscosity. This does not necessarily invalidate all of the previous work, as the general streamline form and concept of the deposition method is yet the same, but the apparent viscosity of the fluid medium has been reduced in proportion to the amount of general turbulence present.

According to Dallavalle's (6) dimensional analysis of a real fluid without a free boundary, we find a dimensionless constant made up of the ratio of inertial forces/frictional forces equal $\frac{\rho V^2}{L} / \frac{\mu V}{L^2} = \frac{\rho LV}{\mu} = R$, the very familiar Reynolds number. Where ρ = the density of the fluid, L is a linear dimension, V is velocity, and μ is the coefficient of

viscosity. With a constant density of the fluid ρ for a given (LV) which is a function of the velocity of flow, shape and size of vessel in contact with it the Reynolds number reflects the effect of viscosity and $R \propto \frac{\rho k}{\mu}$ where k is a constant = (LV).

In studies of particle dynamics we have two distinct criteria for the Reynolds number R involved. One criteria is the R_ρ (Reynolds number of a particle moving through a viscous fluid) and the other is the R_m (Reynolds number or index indicating apparent viscosity of the fluid medium of the particle).

The Reynolds number reflects the amount of destruction of shear forces in a fluid and thus effectively reduces the frictional forces in a fluid. At very high Reynolds numbers we have approximately the perfect fluid used in potential flow theory in which the viscosity is considered zero.

When we consider the resistance to motion of a particle to passage through a fluid medium, we find there are three distinct types of resistance to motion. They are, streamline, intermediate and turbulent.

All three types of resistance can be represented by one equation

$$F_R = \pi D_\rho^2 C \rho K^2/8 \qquad [A]$$

where

F_R = total drag force acting on body, dynes

D_p = diameter of sphere, centimeters

C = overall drag coefficient, dimensionless

ρ = density of dispension medium or fluid, grams/cubic centimeter

u = relative velocity between main body of fluid and particle or body, centimeter/second

μ = viscosity of dispersion medium or fluid, poises

The drag coefficient for the streamline or Stoke's law region is given by $C_s = \frac{24}{R_p}$

R_p for the sphere = $\frac{LV\rho}{\mu} = \frac{D_p u \rho}{\mu}$

This reduces equation [A] to $F_r = 3\pi D_p \mu u$, the familiar Stoke's equation.

For all kinds of motion, an increase in R_p causes a decrease in drag coefficient. However, in a quiescent viscous fluid the R_p is a function of $D_p u \rho/\mu$, that is, the diameter of the particle, relative velocity of medium and particle, density of fluid medium and viscosity of fluid medium.

Dallavalle (6) gives the ranges of the three types of motion and the corresponding range of the drag coefficient C.

(a) streamline motion $10^{-1} < R < 2$, $C_s = \frac{24}{R_p}$

(b) intermediate motion $2 < R < 500$, $C_i = .4 \frac{40}{R_p}$

(c) turbulent motion $500 < R < 10^5$, $C_t = 0.44$

Lapple (8) gives slightly different ranges.

(a) streamline motion R less than .1 to R = 2, $C_s = \frac{24}{R_p}$

(b) intermediate motion $2 < R < 1000$, $C_t = 18.5 / R_p^{.6}$

(c) turbulent motion $1000 < R < 2 \times 10^5$, $C_t = .44$

Referring back to equation [A] we see that the force F_h is a minimum for turbulent flow at R_p >than 1000. We also note that at an R_p of 1000 the empirical value of C_t is .46 and the coefficient for streamline flow would be $C_s = \frac{24}{1000} = .024$ which would yield a force greatly less from equation [A] $F_h = \pi D_p^2 C \rho u^2 / 8$, than does the turbulent flow coefficient C_t. The motion will always be turbulent when this apparent increase of efficiency due to a reduction of value of the coefficient of drag C, because of the manner in which C, a function of R_p is obtained. R_p being $D_p u \rho / \mu$, it can be made large and thus C small by increasing particle size, relative velocity, density of fluid, or by reducing the viscosity. In reducing the drag coefficient C in any manner except by reducing viscosity we see from equation [A] that we greatly increase the drag force F_h. However, another concept may now be brought out that has not been emphasized formerly and is very important in understanding the resistive force of a particle as it moves through a fluid medium. This is brought out by Dallavalle (6) as follows:

> An interesting situation arises with reference to the application of particle dynamics to fluids and may be stated as follows: Suppose a fluid moves with a velocity V in a duct; the motion of this fluid is determined in accordance with the variables stated in equation (2 - 4); now inject into this moving fluid a particle of diameter d having an initial velocity V_p. What is the motion of the particle?

> We observe that Reynolds criteria for pipes which distinguishes turbulent from streamline flow has a value of 2500, where as the value of the criterion for particles is about 1.0, as may be seen in Figure 3. But we must not be led astray by such criteria. Turbulent motion of a particle in a still fluid is a localized condition, while turbulence in a fluid in motion is general. As we have shown, turbulence denotes a destruction of parallel shearing elements in the fluid so that motion becomes a function of fluid density only. Hence, a particle injected into a turbulent fluid behaves as though its Reynolds number, R , is greater than 1.0 even though its true value may actually be less.
>
> In general we may summarize the above in two statements as follows: (1) If a fluid is in streamline motion, the motion of a particle injected into it may be streamline or turbulent, depending on whether the relative velocity between the fluid and the particle is greater or less than 1.0 thus..... (2) If the fluid is in turbulent motion, the motion of a particle injected into it will be turbulent, regardless of the relative velocity between the particle and the fluid.[1]

Discussion of Turbulence in Field Dusting.

Although the degree of turbulence, and thus breakdown in shear forces within the cloud produced by a conventional duster is not at this time known by the author, it is believed that at least under certain conditions it would be considerable. The use of turbulence as a means of decreasing the apparent viscosity of the fluid medium and thus increasing the dynamical catch has not been explicitly stated as an objective in previous literature to the author's knowledge. Brooks (5) indicates that an increase in dynamic catch would be expected by forced turbulence in the foliage. The general

---

[1] Dallavalle. Micrometrics. P. 39.

concept (not necessarily that of Brooks) has been that forced turbulence in the foliage would merely cause more particles to be brought to close proximity of the plant surfaces and thus the inertia would have more chance to carry particles to the surfaces. Turbulence in the sense above considered need not be as microscopic in size of eddies and need not contain the energy of the cloud as would be required to substantially reduce the apparent viscosity of the air. When the boiling in the air dies down the air returns to its former apparent viscosity and will again support particle transport as it would before energizing to turbulence.

The amount of turbulence that is present in dusting practice is probably very low compared to that which could be generated with a tractor mounted duster and proper design of equipment to create this turbulence. Possibly an increase of efficiency could be gained by lower discharge velocities with a higher energy content in the air in the form of turbulence rather than velocity, so that the dust could remain within the plant region for a longer period of time. At present the dust enters the plant region and then leaves again in a matter of seconds. This type of apparent viscosity lowering could greatly enhance the electrical deposition capacities of a dust cloud if it turns out to be mechanically feasible to create this condition.

It is believed that the author's treatment of particle deposition as related in the early part of the test will

serve to increase the understanding of the problem as presented. However, the particle path as calculated would appear to be incorrect by whatever influence the apparent viscosity decrease and the turbulent motion would have upon the path. In all probability there would be a considerable increase in the deviation of the particle from the streamline and thus a greater percentage of inertial catch than was indicated.

The author does not believe that the introduction of a general high level of microscopic turbulence would invalidate the potential flow concept around the collecting surface but would on the contrary enhance it for the action of turbulence is to, in effect, lower the viscosity and thus make more nearly perfect the potential flow concept.

COMPARISON OF ELECTRIC, INERTIAL, AND GRAVITY FIELDS

In any electric field, static or dynamic, the force on the charge q is the vectorial summation $F = qE \oplus qV_n B$ where

F = force on a particle

q = charge on particle

E = field intensity

V_n = velocity normal to direction of magnetic flux

B = magnetic flux density.

Although the fields cannot be considered static in any sense, the force due to the dynamic part of the above equation is almost entirely negligible because of the relatively small velocities and small flux densities. Thus the electric forces available in a charged dust cloud almost entirely originate from the static part of the equation and are equal approximately to F = qE.

The inertial forces available are due altogether to the dynamic phase of the moving dust cloud and are given by the equation F = ma.

The gravity forces are given by F = mg where

g = acceleration of gravity

m = mass gms

W = mg = F in dynes

The electric forces available for a given geometry are entirely dependent on boundary potentials, charge density and charge level on the particle. The boundary conditions have already been prescribed, but we have yet to consider what charge density can be obtained easily with a field type machine and at what place the charge density (always changing) is to be considered. We are interested in the charge density that is available within the region of the plant surfaces. The question of what density of charge is available is not easily answered because heretofore no instrument has been available for indicating the charge density that is made available by a field machine. The charge level on the particle can be calculated for given particle sizes and given charging nozzles when using the ionized field method of charging particles.

Estimation of Charge Density

15 lb/acre on 42 inch rows.

$\frac{43{,}560 \text{ ft}^2/\text{acre}}{3.5 \text{ ft.}}$ 12,500 ft. of row/acre.

For cotton must fill a volume of foliage 2 x 3 x 1 ft. = 6 cu. ft./ft. of row.

Total volume = 6 x 12,500 = 75,000 cu. ft./acre.

Dust concentration in air = $\frac{15 \text{ lb.} \times 454 \text{ gm/lb.}}{75{,}000 \text{ cu. ft.}}$

$= 9.06 \times 10^{-2}$ gms/cu. ft.

$= 5.25 \times 10^{-6}$ gms/cu. in.

$= 3.2 \times 10^{-6}$ gms/cu. cm.

Consider average particle at 15 microns diameter and density $\delta = 2$. There would be $\frac{4}{3}\pi r^3 \times \delta = \frac{4}{3}\pi(7.5 \times 10^{-4})^3 \times 2$

$= 3.54 \times 10^{-9}$ gms/particle

The number of particles per cu. cm. $= \frac{3.2 \times 10^{-6} \text{ gms/cu. cm.}}{3.54 \times 10^{-9} \text{ gms/particle}}$

$= 904$ particles/cu. cm.

Using the ionized field method for charging, the charge level per particle in a field machine will be approximately $\frac{2}{3} 3E_o r^2$ where E_o is the charging field in the nozzle, $\frac{2}{3}$ is the percentage of maximum charge that can be placed on the particle during the time it is in the charging field, the 3 is the a term that takes into account the material of the dust particle, and r is the radius of the dust particle.

Charge per particle with $E_o = 7$ stat volts/cm. All of the above conditions are attainable without difficulty in the field.

$Q = \frac{2}{3} 3E_o r^2 = 2 \times 7 \times (7.5 \times 10^{-4})^2 = 7.87 \times 10^{-6}$ esu/particle

Total charge/cu. cm. of air $= \rho' = 904$ particles $\times 7.87 \times 10^{-6}$ esu/particle

$\rho' = 7.1 \times 10^{-3}$ esu/cu. cm.

Force on a Metal Sphere Within a Cloud for Case III

We calculate the depressing voltage by

$0 = 2/3\ \pi\rho'(b^2 - a^2) - \frac{aV}{a} + \frac{aV}{b}$ .....$\rho = a$

$0 = 2.1 \times 7.1 \times 10^{-3}(45^2 - 1.1^2) - V(1 - \frac{a}{b})$

$V = \frac{30.2}{1 - .025} = 31$ stat volts.

U for grounded sphere $= 2/3\ \pi\rho'(b^2 - \rho^2) - \frac{aV}{\rho} + \frac{a}{b} V$

$\frac{\partial U}{\partial \rho} = -\frac{4}{3}\pi\rho'\rho + \frac{aV}{\rho^2}$

$\frac{\partial U}{\partial \rho} = -E = -\frac{4}{3}\pi(7.1 \times 10^{-3})\ 1.1 + \frac{31}{1.1}$ .. $\rho = a$

$-E = -3.3 \times 10^{-2} + 28.2$..... $\rho = a$

$-E = 28.2$ stat volts/cm.

$|E| = 28.2$ stat volts/cm.

For a 15 micron diameter particle the force is

$F = |E|\ q = 28.2 \times 7.87 \times 10^{-6} = 222 \times 10^{-6}$ dynes.

Force on a Cloud in Finite Cloud Next to Disk

Force on a particle of a uniform cloud of dust of dimensions 4 inches height and 4 inches diameter next to a conducting disk of 4 inches diameter and at zero potential.

Using $\rho' 1938 = \rho$, $7.1 \times 10^{-3} \times 1.938 \times 10^{3} = 13.75$ units/cu. in.

Using maximum intensity as found in previous section as 19.1ρ

$E = 19.1\rho = 19.1 \times 13.75 = 263$ volts/inch

Converting to esu units this is $\frac{263 \text{ volts/inch}}{300 \text{ volts/stat volt} \times 2.54 \text{ cm/in.}}$

$|E| = \frac{263}{764} = .344$ stat volts/cm.

Force on a 15 micron particle at surface of disk is

$F = |E|q = .344 \times 7.87 \times 10^{-6} = 2.71 \times 10^{-6}$ dynes.

The force is toward the disk.

Force on Particle in Cloud Between Two Disks

Calculations for force on a particle along the axis and at the surface of a 4 inch conducting disk when the cloud is sandwiched between two disks as in Figure (22).

Using the same charge density as in the previous cases

ρ = 13.75 units/cu. inch.

The intensity $|E|$ is given as 15.82 ρ

$|E| = 15.82 \times 13.75 = 217$ volts/inch = .285 stat volts/cm.

$F = |E| Q = .285 \times 7.87 \times 10^{-6} = 2.24 \times 10^{-6}$ dynes

The force is toward the disk.

Inertial Force on Particle in Deflected Airstream

Calculation of inertial force on a 20 micron particle of density $\delta = 2$.

From Appendix III

$$x(t) = x_0 + .964 (5 \sin wt - \cos wt) - .036 e^{-\frac{k}{m}t} + 1$$

$$\frac{dx}{dt} = .964 (5 w \cos wt + w \sin wt) + \frac{k}{m} (.036 e^{-\frac{k}{m}t})$$

$$\frac{d^2x}{dt^2} = .964\ (-5\ w^2 \sin wt + w^2 \cos wt) - \frac{k^2}{m^2}(.036\ e^{-\frac{k}{m}t})$$

$$= .964\ (-5w^2) - \frac{(3.78)^2 \times 10^{-12}}{(8.4)^2 \times 10^{-18}} \times 3.6 \times 10^{-2} \times 3.8 \times 10^{-4}$$

$$\frac{d^2x}{dt^2} = -39{,}000 - 2\ \frac{cm}{sec^2} = \text{acceleration}$$

The actual force of inertia of a particle is in the opposite direction to the force that causes the particle to decelerate.

Maximum force of a 20 micron diameter particle having a density of 2 and carried by a circular streamline of 5 cm. radius with streamline velocity of 450 cm/sec. is
$F = ma = 8.4 \times 10^{-9} \times 39 \times 10^{3} = 327 \times 10^{-6}$ dynes.

Gravity Forces on Particle

Gravity force is given by $F = mg$, and for a 15 micron particle of density $\delta = 2$ is

$$F = \frac{4}{3}\pi\delta r^3 g = 3.54 \times 10^{-9}\ \text{gms} \times 980\ \frac{cm}{sec^2}$$

$$F = 3.48 \times 10^{-6}\ \text{dynes}$$

TABLE XVI

COMPARISON OF THE FORCES OF INERTIA, ELECTRIC AND GRAVITY FIELDS

Diam. of Particle	Inertia force	Electric force	Electric force	Electric force	Gravity force
	dynes x 10^{-6}	dynes x 10^{-6}	dynes x 10^{-6}	dynes x 10^{-6}	dynes x 10^{-6}
		A	B	C	
20 microns	327	395	4.82	3.98	8.26
15 microns	$\simeq$ 138	222	2.71	2.24	3.48
10 microns	$\approx$ 41	99	1.20	0.99	1.03
5 microns	$\simeq$ 5.1	25	0.3	0.25	0.13

Inertial force on a particle of density δ = 2 and in an airstream moving at 450 cm/sec and deflected so that the streamlines make a 5 cm. radius arc.

Electric force A - Force at surface of a small sphere within a spherical dust cloud. Case III of the measurement tests.

Electric force B - Force along the perpendicular axis of a disk as in Figure (21) and next to the disk.

Electric force C - Force on particle in a cloud between two disks at disk surface as in Figure (22).

Gravity force - Force of gravity on particle of mass m.

Discussion of Results

The comparison of forces in the chart of Rable XVI was one of the main goals of this thesis. The quantifying of forces was done to enable the research workers to clear up any misconceptions they may have had, to reveal the ways the forces might be varied and to better understand the mechanism of particle deposition in general. This has not been completely accomplished, but it is felt by the author that considerable light has been brought to bear on the problem.

Considering the inertial forces, it is apparent that when an air stream containing dust is directed perpendicular to a surface with sufficient velocity, it is a most powerful force for the deposition of particles of dust. When the dust stream is not directed perpendicular to the surface, the radius r of Appendix III becomes larger and w falls off very rapidly thus greatly lowering the depositing power of the air stream. The electric field forces of Case III of text using $\rho = 7.1 \times 10^{-3}$ yields values comparable in magnitude to the inertial forces.

The results shown here are the author's best estimate of charge density available in a field duster being perhaps a little on the conservative side when using 15 microns as the average diameter to determine number of particles and indirectly charge density. If 7.5 had been used as the average diameter, the charge density would have been twice what it is, all other factors remaining constant. The electric force

available for deposition on a leaf considering a uniform charge density $\rho = 7.1 \times 10^{-3}$ esu/cc yields values that may be considered small when compared to even gravity forces. How then can we account for an increased deposition when using the charged versus uncharged even in those regions that have small leaf spacings that would not allow a sufficient sized cloud to form even the minute force shown in the chart? The answer is not apparent to the writer, but it is to be expected that the charge densities arrange themselves in such fashion that the potentials are nearly constant within the spacings between the leaves. This means that all of the charged dust circulates as close to the boundaries as is possible consistent with the viscosity of the air and thus creates a higher density and larger forces near the surfaces than is indicated by a consideration of a uniform charge density. There is, of course, a possibility that the charge density ρ is unrealistically low, but it would take several times the densities believed reasonable to make the forces highly important. It may be possible that electric forces in conjunction with gravity and inertial forces make the particles adhere better when the foliage is dry due to polarization of waxes on the plant surfaces than would uncharged particles.

There is no question but that the electric forces are very significant on the outer surfaces when the dust cloud blanket is of considerable thickness. In such crops as onions, the small radii of the stalks and relatively open growth

allows substantial electrical forces to develop.

There are at least three ways by which electrical forces can be enhanced to the advantage of dust deposition. They are (1) dense clouds of dust can be blown into the plant region and then recovered after a certain plant exposure, (2) other methods of charging may be used to obtain a higher charge level on each particle such as by contact charging, and (3) a very high voltage machine producing an ionized stream of air in all the plant region can be used to raise the charge density of the inner plant regions while at the same time charging the particles.

The first of the above methods would require a hood and recovery system. The other two methods would require special equipment to produce their higher charge densities. It is always desirable to obtain the highest level possible on each particle since a lesser number of high level particles can give as high an electric field as a large number of low level charged particles. However, the relative movement of any single particle is improved by the condition of high level of charge on the individual particles.

Thermal repulsion, the force on a particle in a temperature gradient may be significant for very small particles when the leaf temperature is considerably higher than the surrounding air. This force acts to prevent deposition when the leaf is hot and aids deposition when the leaf is colder than surrounding air.

APPENDIX I

Development of the Potential Equation of a Grounded Conducting Sphere in a Charged Dust Cloud by Method of Superposition

The method of solution is to calculate the potential throughout the charged spherical cloud then superpose a spherical cloud of smaller size with a negative charge. This will give a hole with no charge in it. The next step is to insert in this hollow cloud a metal sphere of same radius as hole, carrying the charge just necessary to lower the potential to zero at the boundary of the sphere. This charge happens to be equivalent to the potential of the hole before the sphere was inserted times the capacitance of the sphere.

Potential of a Homogeneous Cloud of Charged Dust of Radius b and charge density $\rho = \rho_0$.

Boundary and other conditions:

b = radius of cloud

$\epsilon_1 = \epsilon_2$, ϵ = dielectric constant of medium.

$\rho = \rho_0$, ρ is charge density of cloud.....$\rho < b$

$\rho = 0$.....$\rho > b$

U_i = Potential inside of cloud.....$\rho \leq b$

U_o = Potential outside of cloud.....$\rho \geq b$

$U_i = U_o$ ..... $\rho = b$

$\epsilon_1 \frac{\partial U_i}{\partial \rho} = \epsilon_2 \frac{\partial U_o}{\partial \rho}$ ..... $\rho = b$

$\lim_{\rho \to \infty} U_o = 0$

$\lim_{\rho \to \infty} \rho U = E$

$\nabla^2 U = \frac{1}{\rho^2} \frac{d}{d\rho} \left(\rho^2 \frac{\partial U}{\partial \rho} \right) = - 4\pi \rho_o$ .....Poisson's Equation

$\nabla^2 U = \frac{1}{\rho^2} \frac{d}{d\rho} \left(\rho^2 \frac{\partial U}{\partial \rho} \right) = 0$ .....Laplace's Equation

Math derivation: By starting with Poisson's and Laplace's Equations we develop the potential within a homogeneous dust cloud of charge density ρ_o.

$\nabla^2 U_i = \frac{1}{\rho^2} \frac{d}{d\rho} \left(\rho^2 \frac{\partial U_i}{\partial \rho} \right) = - 4\pi \rho_i$

$\frac{d}{d\rho} \left(\rho^2 \frac{\partial U_i}{\partial \rho} \right) = - 4\pi \rho_o \rho^2$

$\rho^2 \frac{\partial U_i}{\partial \rho} = - \frac{4}{3} \pi \rho_i \rho^3 + C_1$

$\frac{\partial U_i}{\partial \rho} = - \frac{4}{3} \pi \rho_o \rho + \frac{C_1}{\rho^2}$ (1)

$U_i = - \frac{2}{3} \pi \rho_o \rho^2 - \frac{C_1}{\rho} + C_2$ (2)

$$\nabla^2 U_0 = \frac{1}{\rho^2} \frac{d}{d\rho} \left(\rho^2 \frac{\partial U_0}{\partial \rho} \right) = 0$$

$$\frac{d}{d\rho} \left(\rho^2 \frac{\partial U_0}{\partial \rho} \right) = 0$$

$$\rho^2 \frac{\partial U_0}{\partial \rho} = C_3$$

$$\frac{\partial U_0}{\partial \rho} = \frac{C_3}{\rho^2} \qquad (3)$$

$$U_0 = - \frac{C_3}{\rho} + C_4 \qquad (4)$$

From $\lim_{\rho \to \infty} U_0 = 0$, $C_4 = 0$

From $\lim_{\rho \to \infty} \rho U_0 = E$, $C_3 = - E$

E = total charge = Vol x charge density = $\frac{4}{3} \pi b^3 \omega_0$

$$U_0 = \frac{4\pi \omega_0 b^3}{3\rho} \quad \ldots\ldots\ldots\ldots\ldots\ldots \rho \geq b \qquad (4a)$$

$$\frac{\partial U_0}{\partial \rho} = - \frac{4\pi \omega_0 b^3}{3\rho^2} \quad \ldots\ldots\ldots\ldots\ldots\ldots \rho \geq b \qquad (3a)$$

From $\epsilon_1 \frac{\partial U_i}{\partial \rho} = \epsilon_2 \frac{\partial U_0}{\partial \rho}$ $\ldots\ldots\ldots\ldots \rho = b$

$$- \frac{4}{3} \pi \omega_0 \rho + \frac{C_1}{\rho^2} = - \frac{4\pi \omega_0 b^3}{3\rho^2}$$

$C_1 = 0$

From $U_i = U_o$ ..... $\rho = b$

$$-\frac{2}{3}\pi\rho_0 b^2 + C_2 = \frac{4}{3}\pi\rho_0 b^2$$

$$C_2 = 2\pi\rho_0 b^2$$

$$U_i = -\frac{2}{3}\pi\rho_0\rho^2 + 2\pi\rho_0 b^2 \quad \ldots\ldots\ldots 0 \leq \rho \leq b \qquad (2a)$$

$$\frac{\partial U_i}{\partial \rho} = -\frac{4}{3}\pi\rho_0\rho \quad \ldots\ldots\ldots\ldots\ldots 0 \leq \rho \leq b \qquad (1a)$$

Potential Equation of Homogeneous Cloud of Charged Dust of Radius a and Charge density $\rho = -\rho_0$.

From above.

$$U_i = \frac{2}{3}\pi\rho_0\rho^2 - 2\pi\rho_0 a^2 \quad \ldots\ldots\ldots \rho \leq a \qquad (5)$$

$$\frac{\partial U_i}{\partial \rho} = \frac{4}{3}\pi\rho_0\rho \quad \ldots\ldots\ldots\ldots\ldots \rho \leq a \qquad (6)$$

$$U_o = \frac{-4\pi\rho_0 a^3}{3\rho} \quad \ldots\ldots\ldots\ldots\ldots \rho \geq a \qquad (7)$$

$$\frac{\partial U_o}{\partial \rho} = \frac{4\pi\rho_0 a^3}{3\rho^2} \quad \ldots\ldots\ldots\ldots\ldots \rho \geq a \qquad (8)$$

Potential of Hollow Cloud.

The hollow cloud is made up of sum of cloud of radius a and $\rho = -\rho_0$, and cloud of radius b and $\rho = \rho_c$ where $a < b$.

By addition of equations (2a) and (5)

$$U = + 2\pi \rho_0 (b^2 - a^2) \ldots\ldots\ldots\ldots\ldots \rho \leq a \qquad (9)$$

By addition of equation (2a) and (7)

$$U = - \frac{2}{3} \pi \rho_0 \rho^2 + 2\pi \rho_0 b^2 - \frac{4\pi \rho_0 a^3}{3\rho} \ldots a \leq \rho \leq b \qquad (10)$$

By addition of (4a) and (7)

$$U = \frac{4\pi \rho_0 (b^3 - a^3)}{3\rho} \ldots\ldots\ldots\ldots\ldots \rho \geq b \qquad (11)$$

Discussion of System of Grounded Conducting Sphere Inside of Hollow Charged Cloud.

The potential equation of this system is developed by adding the potential of a charged conducting sphere of radius a to the potential of hollow cloud.

The negative of (9) must be put on the conducting sphere to depress the potential of the hole to zero. The charge Q to produce this negative potential is found by the relation $Q = VC$, where Q is the charge, V is the potential and $C = a$ is the capacitance of the conducting sphere*. Therefore, the charge to depress the hole to zero is given by $Q = - 2\pi \rho_0 (b^2 - a^2) a$.

The Potential of the Sphere with Charge Q.

$$Q = - 2\pi \rho_0 (b^2 - a^2) a$$

* The capacitance of a sphere is equal to its radius in unrationalized units.

$$U = \frac{Q}{C} = \frac{Q}{a} = -2\pi\rho_0 (b^2 - a^2) \ldots\ldots\ldots\ldots \rho \leq a \qquad (12)$$

$$U = \frac{Q}{\rho} \quad \frac{- 2\pi\rho_0 (b^2 - a^2) a}{\rho} \ldots\ldots\ldots\ldots \geq a \qquad (13)$$

Potential Equation of Hollow Cloud Containing Grounded Sphere.

By adding equations (9) and (12)

$$U = 0 \ldots\ldots\ldots\ldots\ldots\ldots\ldots\ldots\ldots \rho \leq a \qquad (14)$$

Adding (10) and (13)

$$U = - \frac{2}{3} \pi \rho_0 \rho^2 + 2\pi\rho_0 b^2 \quad \frac{- 4\pi\rho_0 a^3}{3\rho}$$

$$- \frac{2\pi\rho_0 (b^2 - a^2) a}{\rho} \ldots\ldots\ldots\ldots\ldots\ldots a \leq \rho \leq b \qquad (15)$$

By adding (11) and (13)

$$U = \frac{4\pi\rho_0 (b^3 - a^3)}{3\rho} - \frac{2\pi\rho_0 (b^2 - a^2) a}{\rho} \ldots\ldots \rho \geq b \qquad (16)$$

Field Intensity E in Charged Cloud with Grounded Conducting Sphere Inside.

The field intensity is given as the negative of $\frac{\partial U}{\partial \rho}$.

$$- E = \frac{\partial U}{\partial \rho} = 0 \ldots\ldots\ldots\ldots\ldots\ldots\ldots\ldots \rho \leq a \qquad (17)$$

$$- E = \frac{\partial U}{\partial \rho} = \frac{- 4\pi\rho_0 \rho}{3} + \frac{4\pi\rho_0 a^3}{3\rho^2}$$

$$+ \frac{2\pi\rho_0 (b^2 - a^2) a}{\rho^2} \ldots\ldots\ldots\ldots a \leq \rho \leq b \qquad (18)$$

$$- E = \frac{\partial U}{\partial \rho} = - \frac{4\pi\rho_0 (b^3 - a^3)}{3\rho^2} + \frac{2\pi\rho_0 (b^2 - a^2) a}{\rho^2} \ldots \rho \geq b \qquad (19)$$

APPENDIX II

Development of the Potential Equation of a Grounded Conducting Sphere in a Charged Dust Cloud by Method of Inversion in a Sphere

By use of a Kelvin transformation or inversion in a sphere the surface formed by $r = a$ can be made at zero potential, so that the surface charge on the conducting sphere is replaced by a volume distribution within the conducting sphere. The inner boundary will be at $c = a^2/b$ where a is the sphere radius and b is the radius of the dust cloud.

Boundary and Other Conditions.

$U_1 = U_2$, $\epsilon_1 \partial U_1/\partial \rho = \epsilon_2 \partial U_2/\partial \rho$ ..... $\rho = a^2/b$

$U_2 = U_3$, $\epsilon_2 \partial U_2/\partial \rho = \epsilon_3 \partial U_3/\partial \rho$ ..... $\rho = a$

$U_3 = U_4$, $\epsilon_3 \partial U_3/\partial \rho = \epsilon_4 \partial U_4/\partial \rho$ ..... $\rho = b$

$\epsilon_1 = \epsilon_2 = \epsilon_3 = \epsilon_4$, where ϵ = dielectric constants of mediums

$\mathcal{D}_1 = 0$, where $\mathcal{D}$ = charge density of region

$\mathcal{D}_2 = -\mathcal{D}_0 a^5/\rho^5$

$\mathcal{D}_3 = \mathcal{D}_0$

$\mathcal{D}_4 = 0$

$\lim_{\rho \to \infty} U_1 = 0$

$\lim_{\rho \to \infty} \rho U_1 = Q$

$$\nabla^2 U = \frac{1}{\rho^2} \frac{d}{d\rho} \left(\rho^2 \frac{\partial U}{\partial \rho}\right) = - 4\pi\rho, \text{ Poisson's equation} \qquad (1)$$

Mathematical Derivation of Potential Equations.

$U_1 = \frac{C_1}{\rho} + C_2$ from (1)

$U_1 =$ constant, $\therefore C_1 = 0$

$$U_1 = C_2 \qquad (2)$$

$$\frac{\partial U_1}{\partial \rho} = 0 \qquad (3)$$

$$\nabla^2 U_2 = \frac{1}{\rho^2} \frac{d}{d\rho} \left(\rho^2 \frac{\partial U_2}{\partial \rho}\right) = - 4\pi\rho_2 = \frac{4\pi\rho_0 a^5}{\rho^5}, \text{ from (1)}$$

$$\frac{d}{d\rho} \left(\rho^2 \frac{\partial U_2}{\partial \rho}\right) = \frac{4\pi\rho_0 a^5}{\rho^3}$$

$$\rho^2 \frac{\partial U_2}{\partial \rho} = - \frac{2\pi\rho_0 a^5}{\rho^2} + C_3$$

$$\frac{\partial U}{\partial \rho} = - \frac{2\pi\rho_0 a^5}{\rho^4} + \frac{C_3}{\rho^2} \qquad (4)$$

$$U_2 = \frac{2\pi\rho_0 a^5}{3\rho^3} - \frac{C_3}{\rho} + C_4 \qquad (5)$$

$$U_3 = - \frac{2\pi\rho_0 \rho^2}{3} + \frac{C_5}{\rho} + C_6 \text{ from integration of (1)} \qquad (6)$$

$$\frac{\partial U_3}{\partial \rho} = - \frac{4\pi\rho_0 \rho}{3} - \frac{C_5}{\rho^2} \qquad (7)$$

$U_4 = \frac{C_7}{\rho} + C_8$ from integration of (1) (8)

$C_8 = 0$, from consideration of $\lim_{\rho \to \infty} U_4 = 0$

$C_7 = Q$, from consideration of $\lim_{\rho \to \infty} \rho U_4 = Q$

$U_4 = \frac{C_7}{\rho} = \frac{Q}{\rho}$ (8a)

$\frac{\partial U_4}{\partial \rho} = -\frac{Q}{\rho^2}$ (9)

$\epsilon_1 \frac{\partial U_1}{\partial \rho} = \epsilon_2 \frac{\partial U_2}{\partial \rho}$ ..... $\rho = a^2/b$

$0 = -\frac{2\pi \omega_0 b^4}{a^3} + \frac{C_3 b^2}{a^4}$ from above condition

$C_3 = 2\pi \omega_0 b^2 a$

Q = total charge = vol times charge density ω

$$Q = [4\pi\omega \int_{\frac{a^2}{b}}^{a} \rho^2 d\rho]_{\omega = -\omega_0 \frac{a^5}{\rho^5}} + [4\pi\omega \int_{a}^{b} \rho^2 d\rho]_{\omega = \omega_0}$$

$$Q = -4\pi\omega_0 \int_{\frac{a^2}{b}}^{a} \frac{a^5}{\rho^4} d\rho + 4\pi\omega_0 \int_{a}^{b} \rho^2 d\rho$$

$$Q = \frac{2}{3}\pi\omega_0 a^3 + \frac{4}{3}\pi\omega_0 b^3 - 2\pi\omega_0 ab^2$$

$\epsilon_3 \frac{\partial U_3}{\partial \rho} = \epsilon_4 \frac{\partial U_4}{\partial \rho}$ ..... $\rho = b$

$-\frac{4\pi\omega_0 b}{3} - \frac{C_5}{b^2} - \frac{Q}{b^2}$, from above condition

$C_5 = Q - \frac{4}{3}\pi\omega_0 b^3 = \frac{2}{3}\pi\omega_0 a^3 - 2\pi\omega_0 ab^2$

$U_3 = U_4$ ..... $\rho = b$

$$-\frac{2}{3}\pi\mu_0 b^2 + \frac{Q - 4/3\,\pi\mu_0 b^3}{b} + C_6 = \frac{Q}{b}\text{ , from above condition}$$

$$C_6 = 2\pi\mu_0 b^2$$

$$U_1 = U_2 \ldots\ldots\ldots\ldots\ldots\ldots\ldots\ldots\ldots \rho = a^2/b$$

$$C_2 = -\frac{4}{3}\pi\mu_0\frac{b^3}{a} + C_4\text{ , from above equation} \qquad (10)$$

$$U_2 = U_3 \ldots\ldots\ldots\ldots\ldots\ldots\ldots\ldots\ldots \rho = a$$

$$\frac{2}{3}\pi\mu_0 a^2 - 2\pi\mu_0 b^2 + C_4 = 0\text{, from above condition} \qquad (11)$$

Solving (10) and (11) simultaneously

$$C_2 = -\frac{4}{3}\pi\mu_0\frac{b^3}{a} + C_4 \qquad (10)$$

$$0 = \frac{2}{3}\pi\mu_0 a^2 + C_4 - 2\pi\mu_0 b^2 \qquad (11)$$

$$C_2 = -\frac{4}{3}\pi\mu_0\frac{b^3}{a} - \frac{2}{3}\pi\mu_0 a^2 + 2\pi\mu_0 b^2 \qquad (12)$$

By substitution of (12) into (10)

$$C_4 = 2\pi\mu_0 b^2 - \frac{2}{3}\pi\mu_0 a^2$$

$$U_3 = -\frac{2\pi\mu_0\rho^2}{3} + \frac{2\pi\mu_0 a^3}{3\rho} - \frac{2\pi\mu_0 ab^2}{\rho} + 2\pi\mu_0 b^2 \qquad (6a)$$

$$\frac{\partial U_3}{\partial \rho} = -\frac{4\pi\mu_0\rho}{3} - \frac{2\pi\mu_0 a^3}{3\rho^2} + \frac{2\pi\mu_0 ab^2}{\rho^2} \qquad (7a)$$

$$U = \frac{Q}{\rho} = \frac{2\pi\mu_0 a^3}{3\rho} + \frac{4\pi\mu_0 b^3}{3\rho} - \frac{2\pi\mu_0 ab^2}{\rho} \qquad (8b)$$

$$\frac{\partial U_4}{\partial \rho} = -\frac{Q}{\rho^2} = -\frac{2\pi\rho_0 a^3}{3\rho^2} - \frac{4\pi\rho_0 b^3}{3\rho^2} + \frac{2\pi\rho_0 ab^2}{\rho^2} \qquad (9a)$$

Summary of Potential Equations in Inside and Outside of Charged Cloud.

$U = 0$ by definition in a grounded conductor... $\rho \leq a$ (13)

$$U_3 = -\frac{2}{3}\pi\rho_0\rho^2 + 2\pi\rho_0 b^2 - \frac{4\pi\rho_0 a^3}{3\rho} - \frac{2\pi\rho_0(b^2 - a^2)a}{\rho} \text{ inside of cloud.....} a \leq \rho \leq b \qquad (6a)$$

$$U_4 = \frac{4\pi\rho_0(b^3 - a^3)}{3\rho} - \frac{2\pi\rho_0(b^2 - a^2)a}{\rho} \text{ outside of cloud, } \rho \geq b \qquad (8b)$$

Summary of Field Intensity Equations for Grounded Sphere Inside of Charged Dust Cloud.

$$-E = \frac{\partial U}{\partial \rho} = 0 \text{ within conductor.....} \rho \leq a$$

$$-E = \frac{\partial U_3}{\partial \rho} - \frac{4\pi\rho_0\rho}{3} + \frac{4\pi\rho_0 a^3}{3\rho^2} + \frac{2\pi\rho_0(b^2 - a^2)a}{\rho^2} \text{ inside of cloud...} a \leq \rho \leq b \qquad (7a)$$

$$-E = \frac{\partial U_4}{\partial \rho} = -\frac{4\pi\rho_0(b^3 - a^3)}{3\rho^2} + \frac{2\pi\rho_0(b^2 - a^2)a}{\rho^2} \ldots \rho \geq b \qquad (9a)$$

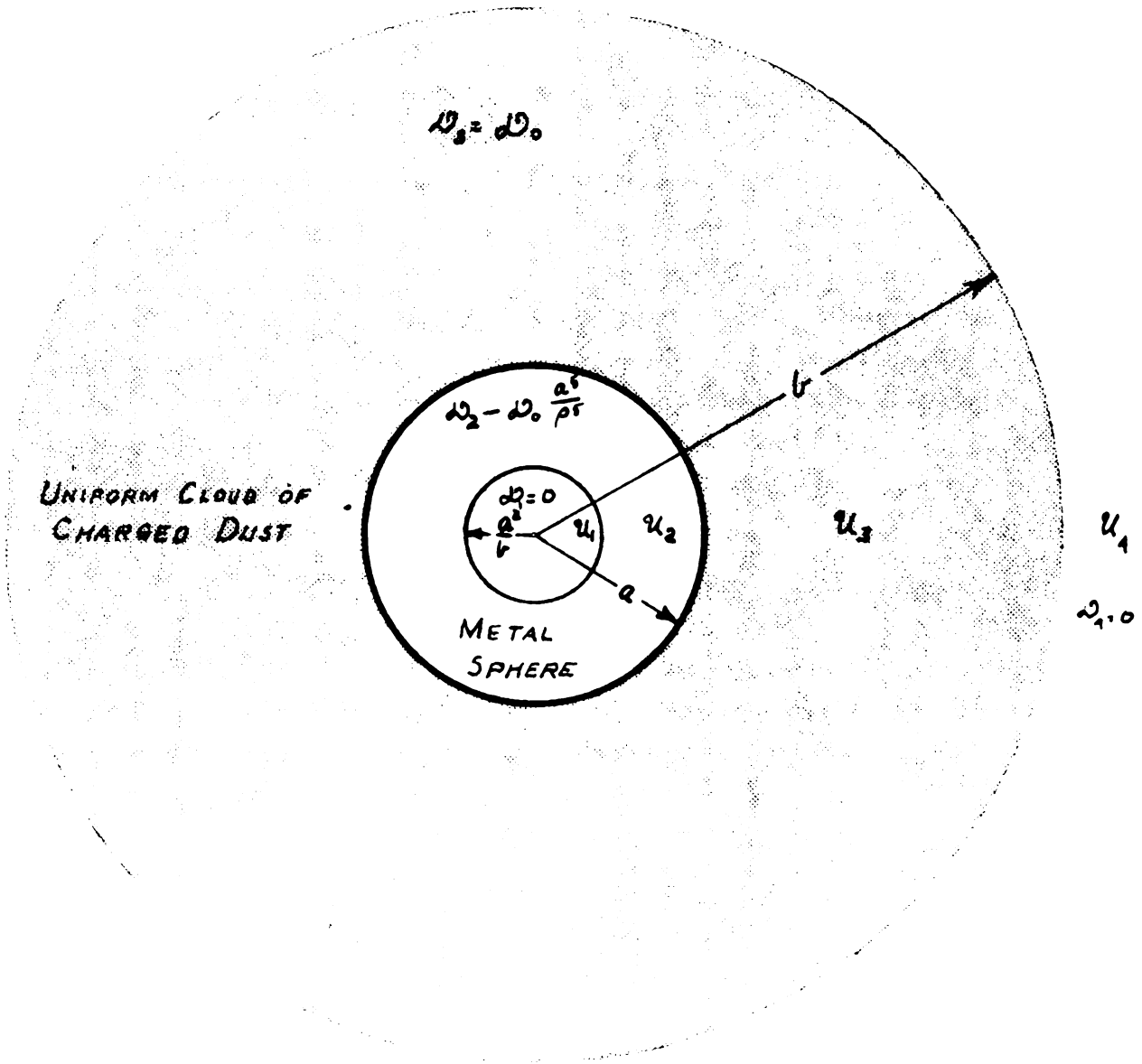

Fig. 52. Cross-section of conducting sphere and cloud showing distribution of charge density as uniform in cloud and non-uniform as imaged into conducting sphere.

APPENDIX III

An Analysis of Particle Deviation from a Circular Streamline

A first approximation to the path of a particle of mass m, having an air drag resistance ku (u = relative velocity particle and air), and subjected to the inertial forces produced on a particle when the particle attempts to follow the streamlines of a deflected air stream may be obtained from the following derivation. A diagram of a circular streamline and relation of co-ordinate system to the streamline is shown in the following figure.

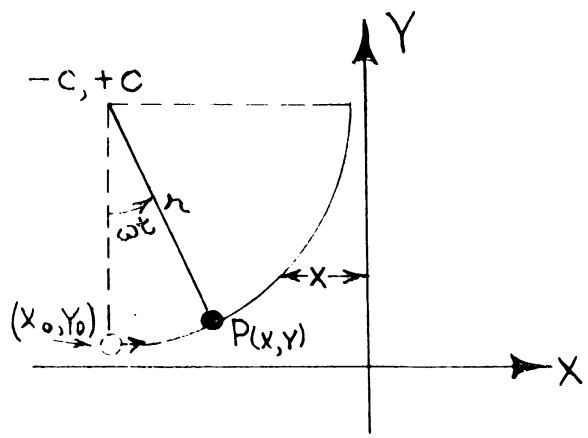

Fig. 53. Co-ordinate System for development of equation on particle deposition by inertial force.

Assumptions and Other Conditions.

The circular streamline equation from the preceding figure is given by

$$x = - C + r \sin wt$$

$$y = + C - r \cos wt$$

The y-axis represents a surface which has deflected a streamline of an impinging airstream into a circular form. The airstream before deflection was directed parallel to the x-axis at a velocity V. Assume that for a given starting position (x_o, y_o) the particle path does not deviate from the streamline circle enough to appreciably change the velocity of the airstream and that the latter velocity is constant, say V_o. It is assumed that at the starting position (x_o, y_o) both the streamline and the particle have the same velocity and direction. Let z = a vector giving the position of a particle P, and V_s = the velocity of the air along a streamline at (x, y).

$M\ddot{z} = k\,(V_s - \dot{z})$ = Drag = k (wind vel. - part. vel.)

$$\ddot{z} + \frac{k}{m}\dot{z} = \frac{k}{m} V_s \qquad (1)$$

The x and y components are given as

$$\ddot{x} + \frac{k}{m}\dot{x} = \frac{k}{m} V_{sx} \qquad (2)$$

$$\ddot{y} + \frac{k}{m}\dot{y} = \frac{k}{m} V_{sy} \qquad (3)$$

$$V_{sx} = \frac{d}{dt}(-C + r \sin wt) = rw \cos wt$$

$$V_{sy} = \frac{d}{dt}(+C - r \cos wt) = rw \sin wt$$

Initial conditions:

$$t = 0,\ x = x_o \tag{4}$$

$$t = 0,\ V_{sx} = \dot{x} = V_o \tag{5}$$

$$t = 0,\ y = y_o \tag{6}$$

$$t = 0,\ V_{sy} = \dot{y} = 0 \tag{7}$$

Mathematical Derivation of Particle Movement in x-direction.

$$\ddot{x} + \frac{k}{m}\dot{x} = + \frac{k}{m} V_{sx}$$

$$\ddot{x} + \frac{k}{m}\dot{x} = + \frac{k}{m} wr \cos wt$$

$$\dot{x}\, e^{\frac{k}{m}t} = + \frac{kwr}{m} \int e^{\frac{k}{m}t} \cos wt$$

$$\dot{x}\, e^{at} = \frac{kwr}{m} \int e^{at} \cos wt$$

$$\dot{x}\, e^{at} = \frac{kwr}{m} \frac{e^{at}}{(w^2 + a^2)} (a \cos wt + w \sin wt) + A$$

$$\dot{x} = \frac{kwr}{m(w^2 + a^2)} (a \cos wt + w \sin wt) + Ae^{-at} \tag{8}$$

$$x = \frac{kwr}{m(w^2 + a^2)} \left(\frac{a}{w} \sin wt - \cos wt\right) - \frac{1}{a} Ae^{-at} + B \tag{9}$$

$t = 0,\ x = x_o,\ \dot{x} = V_o$ (4) and (5)

$$V_o = \frac{kwr}{m(w^2 + a^2)}(a) + A$$

$$A = V_o - \frac{kwra}{m(w^2 + a^2)}$$

$$x_o = \frac{kwr}{m(w^2 + a^2)}(-1) - \frac{V_o}{a} + \frac{kwr}{m(w^2 + a^2)} + B$$

$$B = x_o + \frac{kwr}{m(w^2 + a^2)} + \frac{V_o}{a} - \frac{kwr}{m(w^2 + a^2)}$$

$$B = x_o + \frac{V_o}{a}$$

$$x(t) = \frac{kwr}{m(w^2 + a^2)}\left(\frac{a}{w}\sin wt - \cos wt\right) - \frac{V_o}{a}e^{-at} + \frac{kwr}{m(w^2 + a^2)}e^{-at} + x_o + \frac{V_o}{a} \quad (9a)$$

Mathematical Derivation of Particle Movement in y-direction.

$$\ddot{y} + \frac{k}{m}\dot{y} = \frac{k}{m}V_{sy} \quad (3)$$

$$\ddot{y} + \frac{k}{m}\dot{y} = \frac{k}{m}rw\sin wt$$

$$\dot{y}\,e^{\frac{k}{m}t} = \frac{krw}{m}\int e^{\frac{k}{m}t}\sin wt\,dt$$

$$\dot{y}\,e^{at} = \frac{krw}{m(w^2 + a^2)}\left[e^{at}(a\sin wt - w\cos wt) + A\right] \quad (10)$$

$$y = \frac{krw}{m(w^2 + a^2)}\left(-\frac{a}{w}\cos wt - \sin wt\right) - \frac{1}{a}Ae^{-at} + B \quad (11)$$

$$t = 0,\ \dot{y} = 0 \qquad (7)$$

$$0 = \frac{kwr}{m(w^2 + a^2)}(-w) + A$$

$$A = \frac{krw^2}{m(w^2 + a^2)}$$

$$\text{at } t = 0, \ldots . y = y_o \qquad (6)$$

$$y_o = \frac{krw}{m(w^2 + a^2)}\left(-\frac{a}{w}\right) - \frac{1}{a} \cdot \frac{krw^2}{m(w^2 + a^2)} + B$$

$$B = y_o + \frac{kra}{m(w^2 + a^2)} + \frac{krw^2}{am(w^2 + a^2)}$$

$$y(t) = y_o - \frac{krw}{m(w^2 + a^2)}\left(\frac{a}{w}\cos wt + \sin wt\right) - \frac{1}{a} \cdot \frac{krw^2}{m(w^2 + a^2)} e^{-at}$$

$$+ \frac{kra}{m(w^2 + a^2)} + \frac{krw^2}{am(w^2 + a^2)} \qquad (11a)$$

Evaluation of Constant for a Specific Particle.

$V = 450$ cm/sec = velocity of particle and streamline at $t = 0$

$r = 5$ cm = radius of streamline arc

$w = 90$ radians/sec

$m = 8.4 \times 10^{-9}$ gm = mass of particle

$k = 3.78 \times 10^{-6}$ gm/sec = drag constant = $6\pi\mu R$

$R = 10^{-3}$ cm = particle radius

$\mu \simeq 200 \times 10^{-6}$ poises = viscosity of air

$a = \frac{k}{m} = 4.5 \times 10^2$

$a^2 = \left(\frac{k}{m}\right)^2 = 20.2 \times 10^4$

$$\frac{kwr}{m(w^2 + a^2)} = \frac{3.78 \times 10^{-6} \times .90 \times 10^{2} \times 5}{8.4 \times 10^{-9}(.81 \times 10^{9} + 20.2 \times 10^{9})} = .964 \text{ cm}$$

$$\frac{a}{w} = \frac{450}{5} = 5 \text{ (dimensionless)}$$

$$\frac{wr}{a} = \frac{450}{450} = 1 \text{ cm.}$$

$$\frac{kw^2r}{am(w^2 + a^2)} = \frac{3.78 \times 10^{-6} \times .81 \times 10^{9} \times 5}{450 \times 8.4 \times 10^{-9} \times 21 \times 10^{9}} = .1925 \text{ cm.}$$

$$\frac{akr}{m(w^2 + a^2)} = \frac{.450 \times 10^{3} \times 3.78 \times 10^{-6} \times 5}{17.63 \times 10^{-9}} = 4.83 \text{ cm.}$$

Evaluation of Components of the Particle Path.

The x and y components of the particle path may be found by substituting the constants of the preceding section into the formula for x_ω and y_ω. This is done on the following two pages for four time increments, each corresponding to 22-1/2 degrees of the circular arc. The particle path is found by plotting the x and y components of the path.

TABLE XVII

x-COMPONENT OF PARTICLE PATH

$x(t) = x_o + .964\ (5 \sin wt - \cos wt) - .036\ e^{-\frac{k}{m}t} + 1$

t	wt	sin wt	cos wt	$e^{-\frac{k}{m}t}$	$x_{\bar{o}}$-c	x(t)	x(t) of circle	diff.
0	0	0.000	1	$e^{0} = 1.000$	- 6.0	- 6.0	- 6.0	0
.00437	$22\frac{1}{2}^{o}$	0.383	0.924	$e^{-1.97} = .139$	- 6.0	- 4.01	- 4.08	.07
.00875	45^{o}	0.707	0.707	$e^{-3.94} = .019$	- 6.0	- 2.27	- 2.47	.20
.0131	$67\frac{1}{2}^{o}$	0.924	0.383	$e^{-5.9} = .0027$	- 6.0	- 0.93	- 1.39	.46
.0175	90^{o}	1.000	0.000	$e^{-7.86} = .00038$	- 6.0	- 0.19	- 1.0	.81

Sample calculation: for $x_o = -6$, t = .0175 sec, wt = $\frac{\pi}{2}$ rad,

$x = - 6 + .964\ (5) - .036\ (.00038) + 1$

$x = - 6 + 4.81 - .0000137 + 1 = - 0.19$

TABLE XVIII

y-COMPONENT OF PARTICLE PATH

$y(t) = \mathbf{c} + .0225 - .964\,(5 \cos wt + \sin wt) - .1925\, e^{-\frac{k}{m}t}$

t	wt	sin wt	cos wt	$e^{-\frac{k}{m}t}$	$y_o = \mathbf{c} - r$	y(t)	y(t) of circle	diff.
0	0	0	1	1	1	1	1	0
.00437	$22\frac{1}{2}^o$	.383	.924	$e^{-1.97} = .139$	1	1.16	1.38	.22
.00875	45^o	.707	.707	$e^{-3.94} = .019$	1	1.78	2.47	.69
.0131	$67\frac{1}{2}^o$	.924	.383	$e^{-5.9} = .0027$	1	3.24	4.08	.84
.0175	90^o	1.000	0.000	$e^{-7.86} = .00038$	1	5.06	6.00	.94

Sample calculation: $\mathbf{c} = 6$, $t = .0175$, $wt = \frac{\pi}{2}$ radius

$y = 6.0225 - .964 = 5.06$

APPENDIX IV

Measuring Instruments for Charged Cloud Measurements

The instruments used for electrostatic potential measurements are of two types. The gold leaf electroscope and those depending on the force developed between two charged plates. Both of these types have a variable capacitance, the electroscope having between 3 and 5 cm. and the other types having capacities depending on the design of the instrument. Electrostatic voltmeters do not require continuous current to measure. However, some considerable charge is required to bring these instruments up to potential and this is at the expense of the system being measured. Therefore, care must be exercised in taking results when small systems are being measured. The leads and their position with respect to the surrounding objects and walls of the room effect the capacitance of the total measuring system.

The ordinary Cenco physics laboratory electroscope "A" of Figure (54) is an inexpensive and reliable instrument when a range of 50 to 500 volts is to be measured. They are difficult to use for anything but a reference meter. Certain precautions should be taken if reasonably accurate

results are to be obtained. There is usually about ten to fifteen volts difference in the voltage of a given position of the tip of the gold leaf depending on whether the position is approached from above or below. This is largely due to the bending stress in the gold leaf itself. For more accurate results one should approach a point from the same side as was used for calibrating the meter. The meters are easily calibrated using known sources of d.c. voltage. They read equally well positive or negative electricity and can be used to determine sign of charge by comparing deflection from unknown sign with that of a known sign, such as a comb which is negative after combing through ones hair.

A meter that may be read fairly well from 1000 to 8500 volts, "C" of Figure (54), can easily be constructed from an electroscope, by replacing the gold leaf and suspension with an aluminum foil leaf of double thickness suspended from a pivot shaft and cup bearings from a spring-wound alarm clock. The use of electrostatic voltmeters in charged cloud measurement requires probes and leads. The probes are best made by using a piece of copper or brass that has been coated with an alpha emmitting radioactive salt. Polonium nitrate is relatively easy to obtain and does a very effective job.

The leads are easily made up by stringing a number 36 or 40 enameled copper wire inside a length of spaghetti tubing obtained from a radio shop. The smaller the wire the less capacitance the lead will have. The spaghetti tubing should

have a voltage breakdown rating of at least 8000 volts for use on the high range instrument.

The purpose of the radioactive salt is to emit alpha particles which ionize the air sufficiently in the vicinity of the probe to supply whatever sign of charge is needed to raise the probe and leaf system to the potential of the position of the probe. The charge of sign that does not go on the probe is driven from the probe and tends to lower the potential of the system being measured by whatever amount of opposite sign of ion is used in raising the potential of the probe and instrument movement.

Once the probe has reached the potential of the surroundings the equal number of positive and negative ions formed by action of the radioactive salt will not effect the potential of the system as long as they stay mixed throughout the system in equal numbers. The greater the radioactivity, the faster the instrument can come to the potential of the surroundings. However, this type of sensing element is inherently slow especially with instruments of large electrical capacities.

The small ball on the reference probe for the cloud measurement "A" of Figure (55) and the flat disk on the end of the movable probe "C" of Figure (55) were given four coats each of polonium nitrate.

The suspension and grounding wire for the metal sphere used in Case II, Case III and Case IV of the measured potential test are shown in "B" of Figure (55). The suspension system for the grounded part of the deposit test is shown in

"D" of Figure (55).

The instruments used in tests throughout this thesis are "A" and "B" of Figure (54).

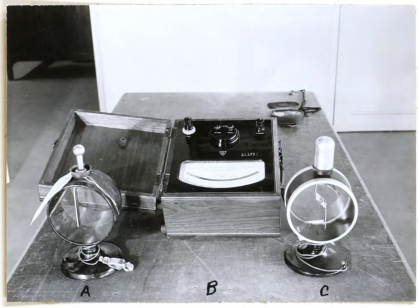

Fig. 54. Instruments for electrostatic potential measured.

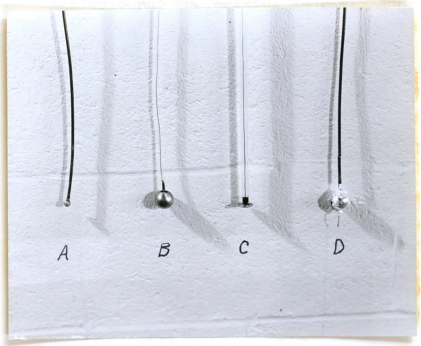

Fig. 55. Probes and suspensions used for the potential measurement and deposit tests.

SELECTED BIBLIOGRAPHY

1. Atwood, Stephen S.
   Electric and Magnetic Fields. 3rd ed. John Wiley and Sons, Inc. New York, 1949. 475 pages

2. Barnes, Neal A.
   Crop Dusting Equipment. Unpublished Progress Report on Research Project. North Carolina State College, Agricultural Engineering Dept., 1951. 26 pages.

3. Bergrun, Norman R.
   A Method for Numerically Calculating the Area and Distribution of Water Impingement on the Leading Edge of an Airfoil in a Cloud. National Advisory Committee for Aeronautics, Washington, D.C., Tech. Note No. 1397. 1947.

4. Bowen, Henry D., Hebblethwaite, Peter, and Carleton, W. M.
   Application of Electrostatic Charging to the Deposition of Insecticides and Fungicides on Plant Surfaces. Agricultural Engineering Journal, June 1952. pp. 347-350.

5. Brooks, F. A.
   The Drifting of Poisonous Dusts Applied by Airplanes and Land Rigs. Agricultural Engineering Journal, June 1947. pp. 233-239.

6. Dallavalle, J. M.
   Micromeritics, The Technology of Fine Particles. 2nd ed. Pitman Publishing Corp. New York and London, 1948. 495 pages.

7. Jeans, Sir James Hopwood
   The Mathematical Theory of Electricity and Magnetism. 5th ed. The University Press. Cambridge, 1933. 645 pages.

8. Lapple, C. E.
   Fluid and Particle Mechanics. University of Delaware. Newark, Del., March 1951. 353 pages.

9. Lapple, C. E. and Shepherd, C. B.
Calculations of Particle Trajectories. Industrial and Engineering Chemistry. Vol. 32, No. 5, 1940. pp. 607-617.

10. Prandtl, L. and Tietjens, O. G.
Translated by J. P. Den Hartog
Applied Hydro and Aeromechanics. 1st ed. McGraw-Hill Book Company, Inc. New York and London, 1934. 306 pages.

11. Prandtl, L. and Tietjens, O. G.
Translated by L. Rosenhead
Fundamentals of Hydro- and Aeromechanics. 1st ed. McGraw-Hill Book Company, Inc. New York and London, 1934. 265 pages.

12. Wilson, E. Bright Jr.
An Introduction to Scientific Research. McGraw-Hill Book Company, Inc. New York, Toronto and London, 1952. 365 pages.